Bias Reduction for an Explicit Solution of Source Localization Using TDOA

K. C. Ho, *Fellow, IEEE*

***Abstract*—This paper proposes two methods to reduce the bias of the well-known algebraic explicit solution (Chan and Ho, "A simple and efficient estimator for hyperbolic location," IEEE Trans. Signal Process., vol. 42, pp. 1905–1915, Aug. 1994) for source localization using TDOA. Bias of a source location estimate is significant when the measurement noise is large and the geolocation geometry is poor. Bias also dominates performance when multiple times of independent measurements are available such as in UWB localization or in target tracking. The paper starts by deriving the bias of the source location estimate from Chan and Ho. The bias is found to be considerably larger than that of the Maximum Likelihood Estimator. Two methods, called BiasSub and BiasRed, are developed to reduce the bias. The BiasSub method subtracts the expected bias from the solution of Chan and Ho's work, where the expected bias is approximated by the theoretical bias using the estimated source location and noisy data measurements. The BiasRed method augments the equation error formulation and imposes a constraint to improve the source location estimate. The BiasSub method requires the exact knowledge of the noise covariance matrix and BiasRed only needs the structure of it. Analysis shows that both methods reduce the bias considerably and achieve the CRLB performance for distant source when the noise is Gaussian and small. The BiasSub method can nearly eliminate the bias and the BiasRed method is able to lower the bias to the same level as the Maximum Likelihood Estimator. The BiasRed method is extended for TDOA and FDOA positioning. Simulations corroborate the performance of the proposed methods.**

***Index Terms*—Bias, localization, FDOA, TDOA.**

I. Introduction

LOCALIZATION of a signal source is a fundamental problem for many applications in radar, sonar, and more recently sensor networks and wireless communications [1]–[11]. Source localization uses a number of spatially separated sensors that measure the emitted or reflected signal from the source. If we are able to model the received signals properly, the direct approach can find the source location by searching all possible positions and selecting the one that best explains the sensor data [12], [13]. Yet an alternative, called the indirect approach here, is to obtain the positioning parameters such as time of arrivals (TOAs) or time differences of arrival (TDOAs) using the signal measurements and deduce from them the location of the source. In the Maximum Likelihood perspective, both approaches yield identical location estimate for Gaussian noise when the signal-to-noise ratio (SNR) of the data measurements is high. At the low SNR region, the direct approach has a higher level of noise tolerance before the thresholding effect occurs. The direct approach, however, requires an accurate model of the received signals and has higher computational complexity than the indirect approach. This paper considers the indirect approach only. In particular we focus on TDOA localization because it is suitable for passive localization and does not require signal time-stamping.

The indirect approach for source localization is less complex but quite challenging. The difficulty comes from the highly nonlinear relationship between the positioning parameters and the unknown. One method to handle the nonlinearity is to use iteration through linearization and [14] provides such a solution using Gauss-Newton implementation of the maximum likelihood estimator (MLE) under Gaussian noise. Such a technique requires carefully chosen initial guesses that are near the actual solution. Convergence is not guaranteed and one could end up with a local minimum solution. Another alternative is to use closed-form solution. Closed-form solution is attractive because it is not iterative and avoids the local convergence problem. [15] derived the explicit constrained least-squares solutions for localization using range or range difference measurements. Least-squares minimization achieves good results when the measurement noise is independent identically distributed (i.i.d.) but the performance degrades if the noise is correlated [16]. For the general case of correlated noise, [1] developed a closed-form solution through nonlinear parameter transformation. It has been shown in both theory and simulation that the solution from [1] reaches the Cramer-Rao lower bound (CRLB) [16] accuracy[1] under Gaussian noise at moderate to high SNR [1], especially when the source is distant. This closed-form solution has been applied to various applications and has often been used as a benchmark for performance comparison in localization algorithm developments, for instance in [17]–[19].

The original closed-form solution proposed in [1] has a much larger amount of bias than the MLE. The large bias is caused by the noise correlation between the regressor and regressand in the formulation for the weighted least-squares (WLS) computation. When the SNR is high or the localization geometry is good, the mean-square location error is dominated by variance and the bias is not observable. This is not the case if the geometry is poor and the SNR is low. Furthermore, modern applications such as ultrawideband (UWB) communications allow multiple independent TDOA measurements to be made at a relatively short time period and several estimates can be averaged together to improve the localization accuracy [17]. Averaging reduces variance and does not decrease bias. In the case of tracking, the measurements at different instants are integrated coherently and the presence of bias is a well-known problem [20]. As a result,

Manuscript received July 05, 2011; revised October 29, 2011; accepted January 18, 2012. Date of publication February 10, 2012; date of current version April 13, 2012. The associate editor coordinating the review of this manuscript and approving it for publication was Dr. Benoit Champagne.

The author is with the Electrical and Computer Engineering Department, University of Missouri, Columbia, MO 65211 USA (e-mail: hod@missouri.edu).

Digital Object Identifier 10.1109/TSP.2012.2187283

[1]CRLB is intended for use with unbiased estimator. It is often used to assess the mean-square error performance of nonlinear estimator as well when the bias resulted from nonlinearity is small compared to variance.

the location bias could limit the performance in poor geometry or in modern localization and tracking applications [17].

To reduce the solution bias of [1], [21] applied a constraint to the unknowns when solving the WLS minimization and it requires numerical search. [17] used the weighted total least-squares (TLS) technique to handle the noise correlation between the regressor and regressand. Although it reduces the bias, the estimation variance is higher than the original solution. [22] also utilized the TLS technique for TDOA localization and [23] for TDOA and frequency difference of arrival (FDOA) localization and they arrived at a similar conclusion as [17].

The paper aims at solving the bias issue of the TDOA location estimate from [1]. To this end, we shall first derive the bias of this solution. Two methods to eliminate the bias will be presented. The first method, denoted by BiasSub, takes the classical approach and subtracts the expected bias from the solution of [1]. The bias subtraction method is effective. It requires, however, the exact knowledge of the TDOA noise power which may not be known in practice. The second method, denoted by BiasRed, creates an augmented solution equation and imposes a quadratic constraint to reduce the bias. The BiasRed solution remains to be in closed explicit form and unlike the BiasSub method it does not require the noise power to be known. Of particular significance is that the BiasRed solution is shown analytically to reach the CRLB accuracy in mean-square position error under Gaussian noise at moderate to high SNR when the source is not close to the sensor array, while maintaining a bias very close to that of the MLE.

Perhaps [17] is the first to examine theoretically the bias of the closed-form solution [1]. We would like to clarify that the bias investigation here is different from that of [17]. Reference [17] derived the bias for the special case of two-dimensional (2D) localization with uncorrelated Gaussian TDOA noise. The bias formula derived here is general and can be applied to 2D or three-dimensional (3D) positioning. In addition, it does not restrict the noise to be uncorrelated. In practice, the TDOA noise is often correlated because the noise in the reference sensor appears in all TDOA values. The proposed solutions are different from previous. First, they are explicit and do not require numerical search as in [21]. Second, they are computationally simple and do not require SVD as in the TLS approach [17]. Third, while the TLS method cannot achieve the CRLB accuracy, the proposed solutions are able to do so at moderate to high SNR when the source is not close to the sensor array. The performance of the proposed solutions is demonstrated by analysis and validated by simulations.

The proposed BiasRed method can be generalized for source localization using other positioning measurements. We shall also provide in this paper the bias-reduced explicit solution for TDOA and FDOA localization [23]–[25].

This paper follows the common notation that bold face upper case letter represents matrix and bold face lower case letter denotes vector. $(*)^o$ is the true value and $(*)$ is its noisy version with additive noise $\Delta(*)$ so that $(*) = (*)^o + \Delta(*)$. $\mathrm{diag}\{\mathbf{a}\}$ is a diagonal matrix formed by the elements of $\mathbf{a}$. The notation $\mathbf{a}(i:j)$ denotes a subvector formed from the ith to the jth element of $\mathbf{a}$ and $\mathbf{A}(i,:)$ represents the ith row of $\mathbf{A}$.

In the next section, we shall summarize the TDOA closed-form solution from [1], provide the bias analysis and introduce the BiasSub method. Section III derives the new BiasRed closed-form solution through augmentation and constrained minimization. Section IV analyzes the BiasRed method and evaluates its bias and variance. Section V extends the BiasRed method for TDOA and FDOA localization. Section VI presents the simulation results and Section VII concludes the paper.

II. Closed-Form Solution and Bias Analysis

We shall consider the scenario in which M spatially separated sensors at locations $\mathbf{s}_i, i = 1,2,\ldots,M$ receive the emitted/reflected signal from a source whose unknown position to be found is $\mathbf{u}^o$. $\mathbf{s}_i$ and $\mathbf{u}^o$ are $N \times 1$ column vectors of Cartesian coordinates, where $N = 2$ for 2D and $N = 3$ for 3D localization. The sensor array computes the relative time delays of the signals at different sensors with respect to the reference, say $\mathbf{s}_1$, to obtain the TDOAs

$$r_{i1} = r_{i1}^o + n_{i1}, \quad i = 2,3,\ldots,M \tag{1}$$

where r_{i1}^o is the true TDOA equal to

$$r_{i1}^o = \|\mathbf{u}^o - \mathbf{s}_i\| - \|\mathbf{u}^o - \mathbf{s}_1\| \tag{2}$$

n_{i1} is the additive noise and $\|*\|$ is the Euclidean norm. Note that (2) is actually the range difference which is the TDOA multiplied by the known signal propagation speed. We shall use time differences and range differences interchangeably throughout the paper because they are differed by a constant scaling factor. The measurement vector is

$$\mathbf{r} = \mathbf{r}^o + \mathbf{n} \tag{3}$$

where $\mathbf{r} = [r_{21}\ r_{31}\ \cdots\ r_{M1}]^T$, $\mathbf{r}^o = [r_{21}^o\ r_{31}^o\ \cdots\ r_{M1}^o]^T$ and $\mathbf{n}$ is zero-mean Gaussian with covariance matrix $\mathbf{Q}$. We are interested in estimating $\mathbf{u}^o$ from $\mathbf{r}$.

A. Closed-Form Solution

The closed-form solution [1] requires at least $N+2$ sensors. The current form presented here assumes the sensors do not lie on a straight line for 2D or a plane for 3D localization. It has a number of stages. The first stage takes the squares of the measurements and introduces the nuisance variable $r_1^o = \|\mathbf{u}^o - \mathbf{s}_1\|$ to obtain a preliminary estimate of $\mathbf{u}^o$ and r_1^o. The second stage improves the estimation accuracy by exploring the relationship between $\mathbf{u}^o$ and r_1^o. The third stage maps the second stage solution to the final position estimate. The equations of the closed-form solution are summarized below and the details of the derivation can be found in [1].

Stage 1:

$$\boldsymbol{\varphi}_1 = \left(\mathbf{G}_1^T\mathbf{W}_1\mathbf{G}_1\right)^{-1}\mathbf{G}_1^T\mathbf{W}_1\mathbf{h}_1 \tag{4}$$

$$\boldsymbol{\varphi}_1 = \begin{bmatrix}\mathbf{u}\\ r_1\end{bmatrix}_{(N+1)\times 1}$$

$$\mathbf{G}_1 = -2\begin{bmatrix}(\mathbf{s}_2-\mathbf{s}_1)^T & r_{21}\\ (\mathbf{s}_3-\mathbf{s}_1)^T & r_{31}\\ \vdots & \vdots\\ (\mathbf{s}_M-\mathbf{s}_1)^T & r_{M1}\end{bmatrix}_{(M-1)\times(N+1)}$$

$$\mathbf{h}_1 = \begin{bmatrix}r_{21}^2 - \mathbf{s}_2^T\mathbf{s}_2 + \mathbf{s}_1^T\mathbf{s}_1\\ r_{31}^2 - \mathbf{s}_3^T\mathbf{s}_3 + \mathbf{s}_1^T\mathbf{s}_1\\ \vdots\\ r_{M1}^2 - \mathbf{s}_M^T\mathbf{s}_M + \mathbf{s}_1^T\mathbf{s}_1\end{bmatrix}_{(M-1)\times 1} \tag{5}$$

$$\mathbf{W}_1 = (\mathbf{B}_1\mathbf{Q}\mathbf{B}_1)^{-1}, \quad \mathbf{B}_1 = 2\,\mathrm{diag}\left\{[r_2^o\ r_3^o\ \cdots\ r_M^o]\right\} \qquad r_i^o = \|\mathbf{u}^o - \mathbf{s}_i\|. \quad (6)$$

Since $\mathbf{B}_1$ contains the true source location and is not known, it is approximated through an initial estimate of $\boldsymbol{\varphi}_1$, say $\hat{\boldsymbol{\varphi}}_1$, when setting $\mathbf{B}_1$ to identity. The ith diagonal element of $\mathbf{B}_1$ is then approximated by $\|\hat{\boldsymbol{\varphi}}_1(1:N) - \mathbf{s}_{i+1}\|$. Alternatively, it can be set to $r_{i+1,1} + \hat{\boldsymbol{\varphi}}_1(N+1)$ which requires less computation.

Stage 2:

$$\boldsymbol{\varphi}_2 = \left(\mathbf{G}_2^T\mathbf{W}_2\mathbf{G}_2\right)^{-1}\mathbf{G}_2^T\mathbf{W}_2\mathbf{h}_2 \quad (7)$$

$$\boldsymbol{\varphi}_2 = (\mathbf{u} - \mathbf{s}_1) \odot (\mathbf{u} - \mathbf{s}_1), \mathbf{G}_2 = \begin{bmatrix} \mathbf{I}_{N\times N} \\ \mathbf{1}_{N\times 1}^T \end{bmatrix}$$

$$\mathbf{h}_2 = \left(\boldsymbol{\varphi}_1 - \begin{bmatrix} \mathbf{s}_1 \\ 0 \end{bmatrix}\right) \odot \left(\boldsymbol{\varphi}_1 - \begin{bmatrix} \mathbf{s}_1 \\ 0 \end{bmatrix}\right) \quad (8)$$

$$\mathbf{W}_2 = \mathbf{B}_2^{-1}\left(\mathbf{G}_1^T\mathbf{W}_1\mathbf{G}_1\right)\mathbf{B}_2^{-1}$$

$$\mathbf{B}_2 = 2\,\mathrm{diag}\left\{\boldsymbol{\varphi}_1 - \begin{bmatrix} \mathbf{s}_1 \\ 0 \end{bmatrix}\right\} \quad (9)$$

where $\odot$ is the operation of element-by-element multiplication.

Stage 3: The final source location estimate is

$$\mathbf{u} = \boldsymbol{\Pi}\sqrt{\boldsymbol{\varphi}_2} + \mathbf{s}_1$$
$$\boldsymbol{\Pi} = \mathrm{diag}\{\mathrm{sgn}(\boldsymbol{\varphi}_1(1:N) - \mathbf{s}_1)\} \quad (10)$$

where $\mathrm{sgn}(*)$ is the signum function.

B. Bias Analysis

The bias analysis here will be up to the second-order statistics of the measurement noise. It assumes the noise level is not large so that the noise terms higher than second order can be ignored. We also require the source is not close to any one of the sensors to ensure $\mathbf{B}_1$ is not sensitive to noise so that it can well be approximated through the procedure described below (6). We shall evaluate the bias at the three stages in sequence.

Bias in $\boldsymbol{\varphi}_1$: Subtracting both sides of the $\boldsymbol{\varphi}_1$ solution (4) by the true value $\boldsymbol{\varphi}_1^o = [\mathbf{u}^{oT},\ r_1^o]^T$ yields

$$\Delta\boldsymbol{\varphi}_1 = \left(\mathbf{G}_1^T\mathbf{W}_1\mathbf{G}_1\right)^{-1}\mathbf{G}_1^T\mathbf{W}_1\left(\mathbf{h}_1 - \mathbf{G}_1\boldsymbol{\varphi}_1^o\right).$$

Using the definitions of $\mathbf{h}_1$ and $\mathbf{G}_1$ from (5) gives the $(i-1)$th element of $\mathbf{h}_1 - \mathbf{G}_1\boldsymbol{\varphi}_1^o$ as $2r_i^o n_{i1} + n_{i1}^2, i = 2, \ldots, M$. In terms of $\mathbf{B}_1$ defined in (6),

$$\Delta\boldsymbol{\varphi}_1 = \left(\mathbf{G}_1^T\mathbf{W}_1\mathbf{G}_1\right)^{-1}\mathbf{G}_1^T\mathbf{W}_1(\mathbf{B}_1\mathbf{n} + \mathbf{n}\odot\mathbf{n}) \quad (11)$$

where $\mathbf{n}$ is the measurement noise vector appeared in (3). Taking expectation yields the bias of $\boldsymbol{\varphi}_1$.

The expectation is not easy to obtain because $\mathbf{G}_1$ defined in (5) contains the noisy TDOA measurements. The Slutsky's theorem [26] that is often used for bias computation is not applicable here because using this theorem requires a large number of sensors or measurements to make $\mathbf{G}_1$ a very tall matrix.

Appendix I evaluates the expectation of (11) and the result is

$$E[\Delta\boldsymbol{\varphi}_1] = \mathbf{H}_1(\mathbf{q} + 2\mathbf{Q}\mathbf{B}_1\mathbf{H}_1(N+1,:)^T) + 2\left(\mathbf{G}_1^{oT}\mathbf{W}_1\mathbf{G}_1^o\right)^{-1}\begin{bmatrix} \mathbf{0}_{N\times 1} \\ \mathrm{tr}\left(\mathbf{W}_1\left(\mathbf{G}_1^o\mathbf{H}_1 - \mathbf{I}\right)\mathbf{B}_1\mathbf{Q}\right) \end{bmatrix} \quad (12)$$

where

$$\mathbf{H}_1 = \left(\mathbf{G}_1^{oT}\mathbf{W}_1\mathbf{G}_1^o\right)^{-1}\mathbf{G}_1^{oT}\mathbf{W}_1 \quad (13)$$

and $\mathbf{H}_1(N+1,:)$ is the last row of $\mathbf{H}_1$. $\mathbf{q}$ is a column vector formed by the diagonal elements of $\mathbf{Q}$ and $\mathrm{tr}(*)$ denotes the trace operation. The first component $\mathbf{H}_1\mathbf{q}$ comes from the second-order noise term in the regressand $\mathbf{h}_1$ due to squaring of the measurements and the remaining components are from the presence of measurement noise in the regressor $\mathbf{G}_1$.

Bias in $\boldsymbol{\varphi}_2$: Subtracting both sides of the $\boldsymbol{\varphi}_2$ solution (7) by the true value $\boldsymbol{\varphi}_2^o$ gives the error

$$\Delta\boldsymbol{\varphi}_2 = \left(\mathbf{G}_2^T\mathbf{W}_2\mathbf{G}_2\right)^{-1}\mathbf{G}_2^T\mathbf{W}_2\left(\mathbf{h}_2 - \mathbf{G}_2\boldsymbol{\varphi}_2^o\right).$$

Using the definition of $\mathbf{h}_2$ and $\mathbf{G}_2$ from (8), $\mathbf{h}_2 - \mathbf{G}_2\boldsymbol{\varphi}_2^o$ can be expressed in terms of $\Delta\boldsymbol{\varphi}_1$ and

$$\Delta\boldsymbol{\varphi}_2 = \left(\mathbf{G}_2^T\mathbf{W}_2\mathbf{G}_2\right)^{-1}\mathbf{G}_2^T\mathbf{W}_2\left(\mathbf{B}_2^o\Delta\boldsymbol{\varphi}_1 + \Delta\boldsymbol{\varphi}_1\odot\Delta\boldsymbol{\varphi}_1\right). \quad (14)$$

The bias and variance of $\Delta\boldsymbol{\varphi}_1$ lead to bias in $\Delta\boldsymbol{\varphi}_2$. Unlike the regressor $\mathbf{G}_1$ in Stage 1, the regressor $\mathbf{G}_2$ is constant and does not have noise. However, $\mathbf{W}_2$ is obtained from $\boldsymbol{\varphi}_1$ through $\mathbf{B}_2$ given in (9). Evaluating the expectation of (14) is not trivial and the details are given in Appendix II.

The bias of $\boldsymbol{\varphi}_2$ is

$$E[\Delta\boldsymbol{\varphi}_2] = \mathbf{H}_2\left(\mathbf{c}_1 + \mathbf{B}_2E[\Delta\boldsymbol{\varphi}_1] + \mathbf{W}_2^{o-1}(\boldsymbol{\alpha} + \boldsymbol{\beta} + \boldsymbol{\gamma})\right) \quad (15)$$

where

$$\mathbf{H}_2 = \left(\mathbf{G}_2^T\mathbf{W}_2^o\mathbf{G}_2\right)^{-1}\mathbf{G}_2^T\mathbf{W}_2^o \quad (16)$$

and $\mathbf{W}_2^o$ is $\mathbf{W}_2$ with $\boldsymbol{\varphi}_1$ replaced by $\boldsymbol{\varphi}_1^o$. $\mathbf{c}_1$ is a column vector containing the diagonal elements of $\mathbf{C}_1$ and $\mathbf{C}_1$ is the mean-square error matrix of $\boldsymbol{\varphi}_1$ which can be approximated by

$$\mathbf{C}_1 = E[(\Delta\boldsymbol{\varphi}_1)(\Delta\boldsymbol{\varphi}_1)^T] = \left(\mathbf{G}_1^{oT}\mathbf{W}_1^o\mathbf{G}_1^o\right)^{-1} + E[\Delta\boldsymbol{\varphi}_1]E[\Delta\boldsymbol{\varphi}_1]^T \approx \left(\mathbf{G}_1^{oT}\mathbf{W}_1\mathbf{G}_1^o\right)^{-1}. \quad (17)$$

$\boldsymbol{\alpha}, \boldsymbol{\beta}$, and $\boldsymbol{\gamma}$ are given in (76)–(78) of Appendix II.

Bias in Final Solution: If we start from the relationship between $\boldsymbol{\varphi}_2$ and $\mathbf{u}$ in (8) and express $\mathbf{u}$ as $\mathbf{u}^o + \Delta\mathbf{u}$ and $\boldsymbol{\varphi}_2$ as $\boldsymbol{\varphi}_2^o + \Delta\boldsymbol{\varphi}_2$, the error in the final solution is

$$\Delta\mathbf{u} = \mathbf{B}_3^{o-1}(\Delta\boldsymbol{\varphi}_2 - \Delta\mathbf{u}\odot\Delta\mathbf{u}) \quad (18)$$

where $\mathbf{B}_3^o = 2\,\mathrm{diag}\{(\mathbf{u}^o - \mathbf{s}_1)\}$. Taking expectation yields

$$E[\Delta\mathbf{u}] \approx \mathbf{B}_3^{o-1}(-\mathbf{c}_u + E[\Delta\boldsymbol{\varphi}_2]) \quad (19)$$

and $\mathbf{c}_u$ is a column vector formed by the diagonal elements of $\mathbf{C}_u$. $\mathbf{C}_u$ is the mean-square error matrix of $\mathbf{u}$ and it can be approximated by the covariance matrix of $\mathbf{u}$ as [1]

$$\mathbf{C}_u \approx \mathbf{B}_3^{o-1}\left(\mathbf{G}_2^T\mathbf{W}_2^o\mathbf{G}_2\right)^{-1}\mathbf{B}_3^{o-1} \quad (20)$$

because the bias of $\Delta\mathbf{u}$ is small compared to its standard deviation.

To summarize, the bias of the closed-form solution is obtained using (12), (15), and (19). It can be approximated by using the estimated source position and the noisy TDOA measurements to replace their true values.

The first method BiasSub simply subtracts the approximated bias from the closed-form solution [1] to remove the bias. Section VI shows that the BiasSub method is quite effective to eliminate the bias. Unfortunately, applying BiasSub requires the noise correlation matrix $\mathbf{Q}$ to be exactly known. Quite often only the structure of the noise covariance matrix is available but not the exact value. For instance, it is proportional to $(\mathbf{I}+\mathbf{1}\mathbf{1}^T)$ for uncorrelated noise in signal measurements of equal SNR [1], where $\mathbf{I}$ is an identity matrix and $\mathbf{1}$ is a vector of unity. In such a case, the BiasSub method will not be applicable.

III. Bias-Reduced Closed-Form Solution

The analysis in Section II indicates the bias in the location estimate of [1] mainly comes from the bias of $\boldsymbol{\varphi}_1$. The second method BiasRed finds a better approach to obtain the Stage 1 solution $\boldsymbol{\varphi}_1$. BiasRed has the advantage over BiasSub in that it only requires the structure of $\mathbf{Q}$. It also avoids the evaluation of the expected bias value which could be tedious.

The derivation starts by adding $r_1^o = \|\mathbf{u}^o - \mathbf{s}_1\|$ on both sides of (1) to obtain $r_{i1} + r_1^o = r_i^o + n_{i1}$. After squaring the two sides and neglecting n_{i1}^2, we arrive at, when collecting all $(M-1)$ equations together for $i = 2, 3, \ldots, M$,

$$\mathbf{B}_1\mathbf{n} = \mathbf{h}_1 - \mathbf{G}_1\boldsymbol{\varphi}_1^o \tag{21}$$

where $\mathbf{B}_1$ is defined in (6), $\mathbf{h}_1$ and $\mathbf{G}_1$ are given in (5) and $\boldsymbol{\varphi}_1^o$ is the true value of $\boldsymbol{\varphi}_1$. The original closed-form solution minimizes

$$\epsilon = (\mathbf{h}_1 - \mathbf{G}_1\boldsymbol{\varphi}_1)^T\mathbf{W}_1(\mathbf{h}_1 - \mathbf{G}_1\boldsymbol{\varphi}_1)$$

to obtain the first stage solution (4).

The BiasRed method introduces the augmented matrix $\mathbf{A}$ and vector $\mathbf{v}$

$$\mathbf{A} = [-\mathbf{G}_1, \mathbf{h}_1], \mathbf{v}^o = \left[\boldsymbol{\varphi}_1^{oT}, 1\right]^T \tag{22}$$

so that (21) and ϵ can be rewritten as

$$\mathbf{B}_1\mathbf{n} = \mathbf{A}\mathbf{v}^o \tag{23}$$

and

$$\epsilon = \mathbf{v}^T\mathbf{A}^T\mathbf{W}_1\mathbf{A}\mathbf{v}. \tag{24}$$

$\mathbf{A}$ contains measurement noise and it is decomposed as

$$\mathbf{A} = \mathbf{A}^o + \Delta\mathbf{A}. \tag{25}$$

$\Delta\mathbf{A}$ is, after subtracting $\mathbf{G}_1$ and $\mathbf{h}_1$ by their true values and ignoring the second-order noise terms in $\mathbf{h}_1$,

$$\begin{aligned}\Delta\mathbf{A} &= 2\left[\mathbf{O}_{(M-1)\times N},\ \mathbf{n},\ \tilde{\mathbf{B}}_1\mathbf{n}\right]\\ \tilde{\mathbf{B}}_1 &= \operatorname{diag}\{[r_{21}^o\ r_{31}^o\ \cdots\ r_{M1}^o]\}\end{aligned} \tag{26}$$

where $\mathbf{O}$ represents a matrix of zeros. Putting (25) into (24) gives the cost function to be minimized as

$$\begin{aligned}\epsilon = \mathbf{v}^T\mathbf{A}^{oT}\mathbf{W}_1\mathbf{A}^o\mathbf{v} + \mathbf{v}^T\Delta\mathbf{A}^T\mathbf{W}_1\Delta\mathbf{A}\mathbf{v}\\ +2\mathbf{v}^T\Delta\mathbf{A}^T\mathbf{W}_1\mathbf{A}^o\mathbf{v}.\end{aligned} \tag{27}$$

The first term on the right-hand side (RHS) is the ideal cost function that reaches the minimum value of 0 at $\mathbf{v} = \mathbf{v}^o$ because $\mathbf{A}^o\mathbf{v}^o = \mathbf{0}$. The noise component $\Delta\mathbf{A}$ perturbs the cost function ϵ, yielding different solutions of $\mathbf{v}$ at different ensembles. Let us take the expectation of ϵ to obtain the cost function on the average

$$E[\epsilon] = \mathbf{v}^T\mathbf{A}^{oT}\mathbf{W}_1\mathbf{A}^o\mathbf{v} + \mathbf{v}^TE[\Delta\mathbf{A}^T\mathbf{W}_1\Delta\mathbf{A}]\mathbf{v}. \tag{28}$$

The third term in (27) vanishes in the expectation since from (26) $\Delta\mathbf{A}$ is zero-mean. Both terms in (28) are nonnegative and dependent on $\mathbf{v}$. When minimizing $E[\epsilon]$ with respect to $\mathbf{v}$, the second term steers the solution away from $\mathbf{v}^o$ and causes bias.

The idea of the BiasRed method is to minimize ϵ subject to the constraint that the second term of (28) is constant. In such a case, $E[\epsilon]$ will attain the minimum value of zero at the true solution $\mathbf{v}^o$. Thus we find $\mathbf{v}$ by

$$\text{minimizing}\quad \mathbf{v}^T\mathbf{A}^T\mathbf{W}_1\mathbf{A}\mathbf{v}\quad \text{subject to}\quad \mathbf{v}^T\boldsymbol{\Omega}\mathbf{v} = k \tag{29}$$

where $\boldsymbol{\Omega} = E[\Delta\mathbf{A}^T\mathbf{W}_1\Delta\mathbf{A}]$. The constant k in the constraint can be any value. Changing its value causes only a different scaling of $\mathbf{v}$ and does not affect the Stage 1 solution $\boldsymbol{\varphi}_1$. Once $\mathbf{v}$ is found, taking its first $(N+1)$ elements and dividing by the last yields $\boldsymbol{\varphi}_1$. A similar approach was used in [27] for bearing-only target motion analysis but the method there requires large number of measurements and no theoretical justification of optimum performance was given.

The constrained minimization problem can be easily solved through the Lagrange multiplier λ and the auxiliary cost function $\mathbf{v}^T\mathbf{A}^T\mathbf{W}_1\mathbf{A}\mathbf{v} + \lambda(k - \mathbf{v}^T\boldsymbol{\Omega}\mathbf{v})$. Taking derivative with respect to $\mathbf{v}$ and setting it to zero yield

$$(\mathbf{A}^T\mathbf{W}_1\mathbf{A})\mathbf{v} = \lambda\boldsymbol{\Omega}\mathbf{v}. \tag{30}$$

Premultiplying by $\mathbf{v}^T$ and using the constraint equality $\mathbf{v}^T\boldsymbol{\Omega}\mathbf{v} = k$, we arrive at $\lambda = \mathbf{v}^T(\mathbf{A}^T\mathbf{W}_1\mathbf{A})\mathbf{v}/k$ which is the cost to be minimized. Hence the solution $\mathbf{v}$ is the generalized eigenvector of the pair $(\mathbf{A}^T\mathbf{W}_1\mathbf{A}, \boldsymbol{\Omega})$ that has the smallest generalized eigenvalue.

The constraint matrix is equal to, after substituting (26),

$$\boldsymbol{\Omega} = E[\Delta\mathbf{A}^T\mathbf{W}_1\Delta\mathbf{A}] = \left[\begin{array}{c|c}\mathbf{O} & \mathbf{O}\\ \hline \mathbf{O} & \tilde{\boldsymbol{\Omega}}\end{array}\right]\begin{matrix}\}N\\ \}2\end{matrix} \tag{31}$$

$$\begin{matrix}\underbrace{\phantom{\mathbf{O}}}_{N} & \underbrace{\phantom{\tilde{\boldsymbol{\Omega}}}}_{2}\end{matrix}$$

and

$$\tilde{\boldsymbol{\Omega}} = 4\begin{bmatrix}\operatorname{tr}(\mathbf{W}_1\mathbf{Q}) & \operatorname{tr}(\mathbf{W}_1\tilde{\mathbf{B}}_1\mathbf{Q})\\ \operatorname{tr}(\tilde{\mathbf{B}}_1\mathbf{W}_1\mathbf{Q}) & \operatorname{tr}(\tilde{\mathbf{B}}_1\mathbf{W}_1\tilde{\mathbf{B}}_1\mathbf{Q})\end{bmatrix} \tag{32}$$

is a 2×2 matrix. The singularity of $\boldsymbol{\Omega}$ is handled by partitioning $\mathbf{v}$ and $\mathbf{A}^T\mathbf{W}_1\mathbf{A}$ into

$$\mathbf{v} = [\underbrace{\mathbf{v}_1^T}_{N}\ \underbrace{\mathbf{v}_2^T}_{2}]^T,\quad \mathbf{A}^T\mathbf{W}_1\mathbf{A} = \left[\begin{array}{cc}\mathbf{A}_{11} & \mathbf{A}_{12}\\ \mathbf{A}_{12}^T & \mathbf{A}_{22}\end{array}\right]\begin{matrix}\}N\\ \}2.\end{matrix}$$

$$\begin{matrix}\underbrace{\phantom{\mathbf{A}_{11}}}_{N} & \underbrace{\phantom{\mathbf{A}_{12}}}_{2}\end{matrix}$$

TABLE I
PROCEDURE FOR OBTAINING THE BIASRED SOLUTION

(i) Create the augmented matrix $\mathbf{A} = [-\mathbf{G}_1,\ \mathbf{h}_1]$.
(ii) Determine $\Delta\mathbf{A} = \mathbf{A} - \mathbf{A}^o$ in terms of the measurement noise.
(iii) Obtain the constraint matrix $\mathbf{\Omega} = E[\Delta\mathbf{A}^T\mathbf{W}_1\Delta\mathbf{A}]$ and partition it into a 2 by 2 block matrix where only the lower right block, denoted by $\tilde{\mathbf{\Omega}}$, is different from zero.
(iv) Partition $\mathbf{A}^T\mathbf{W}_1\mathbf{A}$ in the same form of $\mathbf{\Omega}$ as

$$\mathbf{A}^T\mathbf{W}_1\mathbf{A} = \begin{bmatrix} \mathbf{A}_{11} & \mathbf{A}_{12} \\ \mathbf{A}_{12}^T & \mathbf{A}_{22} \end{bmatrix} \tag{41}$$

where $\mathbf{A}_{22}$ has the same size as $\tilde{\mathbf{\Omega}}$.
(v) Solve $\mathbf{v}_2$ from

$$(\mathbf{A}_{22} - \mathbf{A}_{12}^T\mathbf{A}_{11}^{-1}\mathbf{A}_{12})\mathbf{v}_2 = \lambda\tilde{\mathbf{\Omega}}\mathbf{v}_2\,. \tag{42}$$

(vi) Obtain $\mathbf{v}_1$ using

$$\mathbf{v}_1 = -\mathbf{A}_{11}^{-1}\mathbf{A}_{12}\mathbf{v}_2\,. \tag{43}$$

(vii) Form the Stage 1 solution as

$$\boldsymbol{\varphi}_1 = [\mathbf{v}_1^T,\ \mathbf{v}_2(1:L-1)^T]^T/v_2(L) \tag{44}$$

where L is the length of $\mathbf{v}_2$.
(viii) Continue Stage 2 and Stage 3 processing as in [1] to obtain the final location estimate.

The partitioned form of (30) is

$$\begin{bmatrix} \mathbf{A}_{11}\mathbf{v}_1 + \mathbf{A}_{12}\mathbf{v}_2 \\ \mathbf{A}_{12}^T\mathbf{v}_1 + \mathbf{A}_{22}\mathbf{v}_2 \end{bmatrix} = \begin{bmatrix} \mathbf{0} \\ \lambda\tilde{\mathbf{\Omega}}\mathbf{v}_2 \end{bmatrix} \begin{matrix} \} N \\ \} 2 \end{matrix}. \tag{33}$$

The first N rows gives $\mathbf{v}_1$ in terms of $\mathbf{v}_2$

$$\mathbf{v}_1 = -\mathbf{A}_{11}^{-1}\mathbf{A}_{12}\mathbf{v}_2. \tag{34}$$

Using the above relationship in the last two rows results in

$$\left(\mathbf{A}_{22} - \mathbf{A}_{12}^T\mathbf{A}_{11}^{-1}\mathbf{A}_{12}\right)\mathbf{v}_2 = \lambda\tilde{\mathbf{\Omega}}\mathbf{v}_2. \tag{35}$$

Since $\tilde{\mathbf{\Omega}}$ is positive definite, we can find a unique solution of $\mathbf{v}_2$.

Generalized eigen-decomposition is unnecessary to find $\mathbf{v}_2$ because $\tilde{\mathbf{\Omega}}$ is simply a 2×2 matrix. (35) can be expressed as

$$\mathbf{J}\mathbf{v}_2 = \lambda\mathbf{v}_2 \tag{36}$$

$$\mathbf{J} = \tilde{\mathbf{\Omega}}^{-1}\left(\mathbf{A}_{22} - \mathbf{A}_{12}^T\mathbf{A}_{11}^{-1}\mathbf{A}_{12}\right) = \begin{bmatrix} J_{11} & J_{12} \\ J_{21} & J_{22} \end{bmatrix}. \tag{37}$$

The eigenvalue λ satisfies $\det(\mathbf{J} - \lambda\mathbf{I}) = 0$, where $\det(*)$ represents the determinant of the matrix $(*)$. Hence we have the quadratic equation

$$\lambda^2 - (J_{11} + J_{22})\lambda + J_{11}J_{22} - J_{12}J_{21} = 0$$

and the smaller root is

$$\lambda_{\min} = \frac{1}{2}[(J_{11} + J_{22}) - \sqrt{(J_{11} - J_{12})^2 + 4J_{12}J_{21}}]. \tag{38}$$

Putting $\lambda_{\min}$ back to (36) and setting the second element of $\mathbf{v}_2$ to unity yield, from the second row

$$\mathbf{v}_2 = \left[\left(\frac{\lambda_{\min} - J_{22}}{J_{21}}\right), 1\right]^T. \tag{39}$$

Thus from (34), the first stage solution $\boldsymbol{\varphi}_1$ is

$$\boldsymbol{\varphi}_1 = \left[-\left(\mathbf{A}_{11}^{-1}\mathbf{A}_{12}\mathbf{v}_2\right)^T,\ v_2(1)\right]^T \tag{40}$$

where $v_2(1)$ is the first element of $\mathbf{v}_2$ in (39).

The constraint submatrix $\tilde{\mathbf{\Omega}}$ is given by (32) and it depends on $\tilde{\mathbf{B}}_1$ in (26) that is not known. For implementation purpose the true TDOA values in $\tilde{\mathbf{B}}_1$ are replaced by the measurements and the lost in performance is negligible.

The BiasRed method only changes the computation in Stage 1. The Stage 2 and Stage 3 processing are the same as in the original closed-form solution [1].

The steps to obtain the proposed BiasRed solution is summarized in Table I. In step (v), $\mathbf{v}_2$ is given in (39), where $\mathbf{J}$ and $\lambda_{\min}$ are from (37) and (38). BiasRed can work with any positive definite TDOA noise covariance matrix $\mathbf{Q}$ and does not require the noise to be i.i.d. The solution equation (30) together with (31)–(32) show that a scaling of $\mathbf{Q}$ affects λ and does not change the solution $\mathbf{v}$. Hence BiasRed only needs the structure of $\mathbf{Q}$. We would like to clarify that the constraint matrix $\mathbf{\Omega}$ depends on $\mathbf{W}_1$ which is approximated using the procedure described below (6). The approximation error is less when the source is farther away from the sensor array. Hence the BiasRed method is expected to be more effective for a distant source than a source near or inside the sensor array.

IV. ANALYSIS

This section performs second-order analysis of the BiasRed solution and determines its bias and covariance matrix. The analysis assumes the noise level is not high and the source is not close to any sensors. The first requirement is to guarantee the noise terms higher than second order can be neglected and the second condition is to ensure the error in approximating $\mathbf{W}_1$ by the procedure described below (6) can be ignored. The proposed BiasRed method in Stage 1 solves (29) and its solution is denoted as $\mathbf{v}^*$. $\mathbf{v}^*$ is related to the corresponding Stage 1 solution $\boldsymbol{\varphi}_1^*$ by $\mathbf{v}^*/v^*(N+2) = [\boldsymbol{\varphi}_1^{*T}, 1]^T$, where $v^*(N+2)$ is the last element of $\mathbf{v}^*$. The equation error at this solution is

$$\begin{aligned} \mathbf{A}\mathbf{v}^* &= [-\mathbf{G}_1, \mathbf{h}_1]\begin{bmatrix} \boldsymbol{\varphi}_1^* \\ 1 \end{bmatrix} \\ &= -\mathbf{G}_1^o\boldsymbol{\varphi}_1^* - \Delta\mathbf{G}_1\boldsymbol{\varphi}_1^* + \mathbf{h}_1 \\ &= -\mathbf{G}_1^o\boldsymbol{\varphi}_1^* + \mathbf{h}_1 + 2\varphi_1^*(N+1)\mathbf{n} \end{aligned}$$

where (68) has been used for $\Delta\mathbf{G}_1$ and $\varphi_1^*(N+1)$ is the last element of $\boldsymbol{\varphi}_1^*$. Let us define

$$\check{\mathbf{A}} = [-\mathbf{G}_1^o,\ \mathbf{h}_1 + 2\varphi_1^*(N+1)\mathbf{n}] \tag{45}$$

then

$$\mathbf{A}\mathbf{v}^* = \check{\mathbf{A}}\mathbf{v}^*.$$

We shall simplify the analysis by making the approximation that the solution to (29) is the same as that to the following:

$$\begin{aligned} &\text{minimizing} \quad \mathbf{v}^T\check{\mathbf{A}}^T\mathbf{W}_1\check{\mathbf{A}}\mathbf{v} \\ &\text{subject to} \quad \mathbf{v}^T E[\Delta\check{\mathbf{A}}^T\mathbf{W}_1\Delta\check{\mathbf{A}}]\mathbf{v} = 1. \end{aligned} \tag{46}$$

The solution of (46) satisfies

$$(\check{\mathbf{A}}^T\mathbf{W}_1\check{\mathbf{A}})\mathbf{v}^* = \lambda E[\Delta\check{\mathbf{A}}^T\mathbf{W}_1\Delta\check{\mathbf{A}}]\mathbf{v}^* \tag{47}$$

where λ is the minimum value of ${\mathbf{v}^*}^T\check{\mathbf{A}}^T\mathbf{W}_1\check{\mathbf{A}}\mathbf{v}^*$. The analysis continues by obtaining $\Delta\check{\mathbf{A}}$ and deriving the property of $\mathbf{v}^*$ from (47).

$\Delta\check{\mathbf{A}}$ is equal to $\check{\mathbf{A}} - \check{\mathbf{A}}^o$, where $\check{\mathbf{A}}^o = [-\mathbf{G}_1^o,\ \mathbf{h}_1^o]$. $\mathbf{h}_1$ is defined in (5) and hence

$$\mathbf{h}_1 = \mathbf{h}_1^o + 2\tilde{\mathbf{B}}_1\mathbf{n} + \mathbf{n}\odot\mathbf{n} \tag{48}$$

where $\tilde{\mathbf{B}}_1$ is defined in (26). As a result

$$\Delta\check{\mathbf{A}} = \left[\mathbf{O}_{(M-1)\times(N+1)},\ 2\tilde{\mathbf{B}}_1\mathbf{n} + \mathbf{n}\odot\mathbf{n} + 2\varphi_1^*(N+1)\mathbf{n}\right].$$

The constraint matrix of (46) simplifies to

$$E[\Delta\check{\mathbf{A}}^T\mathbf{W}_1\Delta\check{\mathbf{A}}] = \underbrace{\left[\begin{array}{c|c}\mathbf{O} & \mathbf{0}^T \\ \hline \mathbf{0} & \{*\}\end{array}\right]}_{\begin{matrix}N+1 & 1\end{matrix}}\begin{matrix}\}N+1\\ \}1\end{matrix} \tag{49}$$

where $\{*\}$ is a scalar whose value is not relevant in the analysis.

The partition of $\check{\mathbf{A}}^T\mathbf{W}_1\check{\mathbf{A}}$ in the same form as (49) is, upon using (45), we obtain (50) (shown at the bottom of the page). Putting (49) and (50) into (47), the first $N+1$ entries satisfy

$$\left[{\mathbf{G}_1^o}^T\mathbf{W}_1\mathbf{G}_1^o, -{\mathbf{G}_1^o}^T\mathbf{W}_1\left(\mathbf{h}_1 + 2\varphi_1^*(N+1)\mathbf{n}\right)\right]\mathbf{v}^* = \mathbf{0}.$$

Dividing it by $v^*(N+2)$ and using $\mathbf{v}^*/v^*(N+2) = [{\boldsymbol{\varphi}_1}^{*T}, 1]^T$ yield

$$\left({\mathbf{G}_1^o}^T\mathbf{W}_1\mathbf{G}_1^o\right){\boldsymbol{\varphi}_1}^* - {\mathbf{G}_1^o}^T\mathbf{W}_1(\mathbf{h}_1 + 2\varphi_1^*(N+1)\mathbf{n}) = \mathbf{0}. \tag{51}$$

Since $\mathbf{h}_1^o = \mathbf{G}_1^o\boldsymbol{\varphi}_1^o$ and $\varphi_1^o(N+1) = r_1^o$, applying (48) gives

$$\begin{aligned} &\mathbf{h}_1 + 2\varphi_1^*(N+1)\mathbf{n} \\ &\quad = \mathbf{G}_1^o\boldsymbol{\varphi}_1^o + 2\tilde{\mathbf{B}}_1\mathbf{n} \\ &\qquad + \mathbf{n}\odot\mathbf{n} + 2r_1^o\mathbf{n} + 2\Delta\varphi_1^*(N+1)\mathbf{n} \\ &\quad = \mathbf{G}_1^o\boldsymbol{\varphi}_1^o + \mathbf{B}_1\mathbf{n} + \mathbf{n}\odot\mathbf{n} + \left[\mathbf{O}_{(M-1)\times N}, 2\mathbf{n}\right]\Delta\boldsymbol{\varphi}_1^* \end{aligned}$$

where $\Delta\boldsymbol{\varphi}_1^* = \boldsymbol{\varphi}_1^* - \boldsymbol{\varphi}_1^o$ is the error of $\boldsymbol{\varphi}_1^*$ with respect to the true value, $2\tilde{\mathbf{B}}_1 + 2r_1^o\mathbf{I} = \mathbf{B}_1$ has been used and $\mathbf{B}_1$ is defined in (6). As a result, (51) becomes

$$(\mathbf{I} - [\mathbf{O}, 2\mathbf{H}_1\mathbf{n}])\Delta\boldsymbol{\varphi}_1^* = \mathbf{H}_1(\mathbf{B}_1\mathbf{n} + \mathbf{n}\odot\mathbf{n})$$

where $\mathbf{H}_1$ is defined in (13). When the noise level is not large, the approximation $(\mathbf{I} - [\mathbf{O},\ 2\mathbf{H}_1\mathbf{n}])^{-1} \approx \mathbf{I} + [\mathbf{O},\ 2\mathbf{H}_1\mathbf{n}]$ is valid [28] and

$$\begin{aligned} \Delta\boldsymbol{\varphi}_1^* &\approx (\mathbf{I} + [\mathbf{O},\ 2\mathbf{H}_1\mathbf{n}])\mathbf{H}_1(\mathbf{B}_1\mathbf{n} + \mathbf{n}\odot\mathbf{n}) \\ &\approx \mathbf{H}_1\mathbf{B}_1\mathbf{n} + \mathbf{H}_1(\mathbf{n}\odot\mathbf{n}) + [\mathbf{O},\ 2\mathbf{H}_1\mathbf{n}](\mathbf{H}_1\mathbf{B}_1\mathbf{n}). \end{aligned} \tag{52}$$

The noise vector $\mathbf{n}$ is zero mean with covariance $\mathbf{Q}$. The expectation of (52) gives the bias

$$E[\Delta\boldsymbol{\varphi}_1^*] \approx \mathbf{H}_1(\mathbf{q} + 2\mathbf{Q}\mathbf{B}_1\mathbf{H}_1(N+1,:)^T). \tag{53}$$

If we keep only the first-order noise term in (52), multiplying by its transpose yields the covariance

$$E\left[\Delta\boldsymbol{\varphi}_1^*\Delta{\boldsymbol{\varphi}_1^*}^T\right] \approx \mathbf{H}_1\mathbf{B}_1\mathbf{Q}\mathbf{B}_1\mathbf{H}_1^T = \left({\mathbf{G}_1^o}^T\mathbf{W}_1\mathbf{G}_1^o\right)^{-1} \tag{54}$$

where the definitions of $\mathbf{H}_1$ and $\mathbf{W}_1$ in (13) and (6) have been used.

The bias of $\boldsymbol{\varphi}_1$ from BiasRed is (53). Comparing it with (12) of the original solution [1] indicates that BiasRed does not have the last bias component caused by the noise correlation between $\mathbf{G}_1$ and $\mathbf{h}_1$. BiasRed does not increase the covariance matrix of $\boldsymbol{\varphi}_1$ and (54) is the same as in the original closed-form solution.

The bias of the final location estimate is obtained from (19), where $E[\Delta\boldsymbol{\varphi}_1]$ in (15) is (53). This is because BiasRed only modifies the solution of Stage 1 and the processing in Stage 2 and Stage 3 remains to be the same as before. (54) is the covariance of $\boldsymbol{\varphi}_1$ used in [1] to prove that the performance achieves the CRLB accuracy for small Gaussian noise and distant source far from the sensors. Consequently, BiasRed maintains the mean-square performance as the original solution [1] while having smaller bias. The simulation in Section VI shows that BiasRed indeed lowers the bias to the same level as the MLE.

V. Bias Reduction for TDOA and FDOA Localization

The proposed BiasRed method is applicable to other closed-form solutions that use different positioning measurements such as TOA and FDOA. We shall illustrate the use of this technique for TDOA and FDOA positioning [24].

The localization problem is to estimate the position $\mathbf{u}^o$ and the velocity $\dot{\mathbf{u}}^o$ of a moving object, using M mobile sensors at known positions $\mathbf{s}_i$ and velocities $\dot{\mathbf{s}}_i, i = 1, 2, \ldots, M$. In addition to TDOAs given in (3), we also have FDOAs

$$\dot{\mathbf{r}} = \dot{\mathbf{r}}^o + \dot{\mathbf{n}} \tag{55}$$

$$\check{\mathbf{A}}^T\mathbf{W}_1\check{\mathbf{A}} = \begin{bmatrix} {\mathbf{G}_1^o}^T\mathbf{W}_1\mathbf{G}_1^o & -{\mathbf{G}_1^o}^T\mathbf{W}_1(\mathbf{h}_1 + 2\varphi_1^*(N+1)\mathbf{n}) \\ -(\mathbf{h}_1 + 2\varphi_1^*(N+1)\mathbf{n})^T\mathbf{W}_1\mathbf{G}_1^o & (\mathbf{h}_1 + 2\varphi_1^*(N+1)\mathbf{n})^T\mathbf{W}_1(\mathbf{h}_1 + 2\varphi_1^*(N+1)\mathbf{n}) \end{bmatrix}. \tag{50}$$

where $\dot{\mathbf{r}} = [\dot{r}_{21}\ \dot{r}_{31}\ \ldots\ \dot{r}_{M1}]^T, \dot{\mathbf{r}}^o = [\dot{r}^o_{21}\ \dot{r}^o_{31}\ \ldots\ \dot{r}^o_{M1}]^T$ and $\dot{\mathbf{n}}$ is the noise. The FDOAs have been converted to the range rate differences through multiplying by the signal propagation speed and dividing by the center frequency. FDOA is related to the source position and velocity by [24]

$$\dot{r}^o_{i1} = \frac{1}{\|\mathbf{u}^o - \mathbf{s}_i\|}(\mathbf{u}^o - \mathbf{s}_i)^T(\dot{\mathbf{u}}^o - \dot{\mathbf{s}}_i) - \frac{1}{\|\mathbf{u}^o - \mathbf{s}_1\|}(\mathbf{u}^o - \mathbf{s}_1)^T(\dot{\mathbf{u}}^o - \dot{\mathbf{s}}_1). \quad (56)$$

The composite measurement vector is

$$\mathbf{m} = [\mathbf{r}^T,\ \dot{\mathbf{r}}^T]^T.$$

The corresponding noise vector is $\mathbf{n}_m = [\mathbf{n}^T, \dot{\mathbf{n}}^T]^T$ and it is modeled as zero-mean Gaussian with covariance matrix

$$\mathbf{Q} = E[\mathbf{n}_m\mathbf{n}_m^T] = \begin{bmatrix} \mathbf{Q}_r & \mathbf{Q}_{r\dot{r}} \\ \mathbf{Q}_{r\dot{r}}^T & \mathbf{Q}_{\dot{r}} \end{bmatrix}.$$

We are interested in estimating the source position $\mathbf{u}^o$ and velocity $\dot{\mathbf{u}}^o$, using the TDOAs and FDOAs.

The closed-form solution for TDOA and FDOA positioning was derived in [24] and will not be repeated here for brevity. The original solution has much larger location (position and velocity) bias than the MLE, where the large bias is due to the noise correlation between $\mathbf{G}_1$ and $\mathbf{h}_1$ in the Stage 1 processing.

We shall present the proposed solution by applying the BiasRed technique summarized in Table I. It has three stages. The changes are in Stage 1, and the processing in Stage 2 and Stage 3 is the same as in [24].

Stage 1: Let us first define the Stage 1 unknown vector $\boldsymbol{\varphi}_1$ and the matrices $\mathbf{G}_1$ and $\mathbf{h}_1$ as

$$\boldsymbol{\varphi}_1 = \begin{bmatrix} \mathbf{u} \\ \dot{\mathbf{u}} \\ r_1 \\ \dot{r}_1 \end{bmatrix}$$

$$\mathbf{G}_1 = -2\begin{bmatrix} (\mathbf{s}_2 - \mathbf{s}_1)^T & \mathbf{0}^T & r_{21} & 0 \\ & \vdots & & \\ (\mathbf{s}_M - \mathbf{s}_1)^T & \mathbf{0}^T & r_{M1} & 0 \\ \hline (\dot{\mathbf{s}}_2 - \dot{\mathbf{s}}_1)^T & (\mathbf{s}_2 - \mathbf{s}_1)^T & \dot{r}_{21} & r_{21} \\ & \vdots & & \\ \underbrace{(\dot{\mathbf{s}}_M - \dot{\mathbf{s}}_1)^T}_{N} & \underbrace{(\mathbf{s}_M - \mathbf{s}_1)^T}_{N} & \dot{r}_{M1} & r_{M1} \end{bmatrix} \begin{matrix} \left.\vphantom{\begin{matrix}a\\b\\c\end{matrix}}\right\} M-1 \\ \left.\vphantom{\begin{matrix}a\\b\\c\end{matrix}}\right\} M-1 \end{matrix}$$

$$\mathbf{h}_1 = \begin{bmatrix} r_{21}^2 - \mathbf{s}_2^T\mathbf{s}_2 + \mathbf{s}_1^T\mathbf{s}_1 \\ \vdots \\ r_{M1}^2 - \mathbf{s}_M^T\mathbf{s}_M + \mathbf{s}_1^T\mathbf{s}_1 \\ \hline 2(r_{21}\dot{r}_{21} - \mathbf{s}_2^T\dot{\mathbf{s}}_2 + \mathbf{s}_1^T\dot{\mathbf{s}}_1) \\ \vdots \\ 2(r_{M1}\dot{r}_{M1} - \mathbf{s}_M^T\dot{\mathbf{s}}_M + \mathbf{s}_1^T\dot{\mathbf{s}}_1) \end{bmatrix} \begin{matrix} \left.\vphantom{\begin{matrix}a\\b\\c\end{matrix}}\right\} M-1 \\ \left.\vphantom{\begin{matrix}a\\b\\c\end{matrix}}\right\} M-1 \end{matrix}. \quad (57)$$

Also, define the weighting matrix [see (58) at the bottom of the page], $\mathbf{W}_1$ is generated in the same manner as in [24] by first setting $\mathbf{B}_1$ to identity and obtaining a preliminary WLS solution of $\hat{\boldsymbol{\varphi}}_1$. The diagonal elements of $\mathbf{B}_{11}$ and $\dot{\mathbf{B}}_{11}$ are set to be $2\|\hat{\boldsymbol{\varphi}}_1(1:N) - \mathbf{s}_{i+1}\|$ and $2(\hat{\boldsymbol{\varphi}}_1(1:N) - \mathbf{s}_{i+1})^T(\hat{\boldsymbol{\varphi}}_1(N+1:2N) - \dot{\mathbf{s}}_{i+1})/\|\hat{\boldsymbol{\varphi}}_1(1:N) - \mathbf{s}_{i+1}\|$.

The augmented matrix $\mathbf{A}$ is

$$\mathbf{A} = [-\mathbf{G}_1, \mathbf{h}_1]_{2(M-1)\times(2N+3)}.$$

After subtracting the true value $\mathbf{A}^o$, $\Delta\mathbf{A}$ is equal to

$$\Delta\mathbf{A} = 2[\mathbf{O}_{2(M-1)\times 2N},\ \mathbf{n}_m,\ \mathbf{E}_{11}\mathbf{n}_m,\ \mathbf{E}_{12}\mathbf{n}_m] \quad (59)$$

$$\mathbf{E}_{11} = \begin{bmatrix} \mathbf{O}_{M-1} & \mathbf{O}_{M-1} \\ \mathbf{I}_{M-1} & \mathbf{O}_{M-1} \end{bmatrix}, \quad \mathbf{E}_{12} = \begin{bmatrix} \tilde{\mathbf{B}}_{11} & \mathbf{O}_{M-1} \\ \dot{\tilde{\mathbf{B}}}_{11} & \tilde{\mathbf{B}}_{11} \end{bmatrix}$$

$$\tilde{\mathbf{B}}_{11} = \operatorname{diag}\{[r^o_{21}\ r^o_{31}\ \cdots\ r^o_{M1}]\},$$

$$\dot{\tilde{\mathbf{B}}}_{11} = \operatorname{diag}\{[\dot{r}^o_{21}\ \dot{r}^o_{31}\ \cdots\ \dot{r}^o_{M1}]\}$$

where the second-order noise term has been ignored, and $\mathbf{O}_{M-1}$ and $\mathbf{I}_{M-1}$ are $(M-1)\times(M-1)$ square matrices of zero and identity. The constraint matrix is [see (60)-(61) at the bottom of the next page]. The partition of $\mathbf{A}^T\mathbf{W}_1\mathbf{A}$ in the same form as $\boldsymbol{\Omega}$ gives the $2N\times 2N$ matrix $\mathbf{A}_{11}$, the $2N\times 3$ matrix $\mathbf{A}_{12}$ and the 3×3 matrix $\mathbf{A}_{22}$. $\mathbf{v}_2$ has a length of 3 and (42) can be solved explicitly without requiring the generalized eigen-decomposition as shown in Appendix III. $\mathbf{v}_1$ is found using (43) and the improved Stage 1 solution is (44).

Stage 2:

$$\boldsymbol{\varphi}_2 = \left(\mathbf{G}_2^T\mathbf{W}_2\mathbf{G}_2\right)^{-1}\mathbf{G}_2^T\mathbf{W}_2\mathbf{h}_2 \quad (62)$$

where

$$\boldsymbol{\varphi}_2 = \begin{bmatrix} (\mathbf{u} - \mathbf{s}_1) \odot (\mathbf{u} - \mathbf{s}_1) \\ (\mathbf{u} - \mathbf{s}_1) \odot (\dot{\mathbf{u}} - \dot{\mathbf{s}}_1) \end{bmatrix}$$

$$\mathbf{G}_2 = \begin{bmatrix} \mathbf{I}_N & \mathbf{O}_N \\ \mathbf{O}_N & \mathbf{I}_N \\ \mathbf{1}^T_{N\times 1} & \mathbf{0}^T_{N\times 1} \\ \mathbf{0}^T_{N\times 1} & \mathbf{1}^T_{N\times 1} \end{bmatrix}$$

$$\mathbf{h}_2 = \begin{bmatrix} (\boldsymbol{\varphi}_1(1:N) - \mathbf{s}_1) \odot (\boldsymbol{\varphi}_1(1:N) - \mathbf{s}_1) \\ (\boldsymbol{\varphi}_1(1:N) - \mathbf{s}_1) \odot (\boldsymbol{\varphi}_1(N+1:2N) - \dot{\mathbf{s}}_1) \\ \varphi_1(2N+1)^2 \\ \varphi_1(2N+1)\varphi_1(2N+2) \end{bmatrix} \quad (63)$$

and the weighting matrix is

$$\mathbf{W}_2 = \mathbf{B}_2^{-T}\left(\mathbf{G}_1^T\mathbf{W}_1\mathbf{G}_1\right)^{-1}\mathbf{B}_2^{-1}$$

$$\mathbf{B}_2 = \begin{bmatrix} 2\mathbf{B}_{22} & \mathbf{O}_{M-1} \\ \dot{\mathbf{B}}_{22} & \mathbf{B}_{22} \end{bmatrix}$$

$$\mathbf{B}_{22} = \operatorname{diag}\left\{\left(\begin{bmatrix} \boldsymbol{\varphi}_1(1:N) \\ \varphi_1(2N+1) \end{bmatrix} - \begin{bmatrix} \mathbf{s}_1 \\ 0 \end{bmatrix}\right)\right\}$$

$$\dot{\mathbf{B}}_{22} = \operatorname{diag}\left\{\left(\begin{bmatrix} \boldsymbol{\varphi}_1(N+1:2N) \\ \varphi_1(2N+2) \end{bmatrix} - \begin{bmatrix} \dot{\mathbf{s}}_1 \\ 0 \end{bmatrix}\right)\right\}. \quad (64)$$

$$\mathbf{W}_1 = \mathbf{B}_1^{-T}\mathbf{Q}^{-1}\mathbf{B}_1^{-1}, \quad \mathbf{B}_1 = \begin{bmatrix} \mathbf{B}_{11} & \mathbf{O}_{M-1} \\ \dot{\mathbf{B}}_{11} & \mathbf{B}_{11} \end{bmatrix}, \quad \begin{matrix} \mathbf{B}_{11} = 2\operatorname{diag}\{[r^o_2\ r^o_3\ \cdots\ r^o_M]\} \\ \dot{\mathbf{B}}_{11} = 2\operatorname{diag}\{[\dot{r}^o_2\ \dot{r}^o_3\ \cdots\ \dot{r}^o_M]\} \end{matrix}. \quad (58)$$

Stage 3:

$$\begin{aligned}\mathbf{u} &= \mathbf{\Pi}\sqrt{\boldsymbol{\varphi}_2(1:N)} + \mathbf{s}_1 \\ \mathbf{\Pi} &= \mathrm{diag}\{\mathrm{sgn}(\boldsymbol{\varphi}_1(1:N) - \mathbf{s}_1)\} \\ \dot{\mathbf{u}} &= \boldsymbol{\varphi}_2(N+1:2N) \cdot /(\mathbf{u} - \mathbf{s}_1)\end{aligned} \tag{65}$$

where $\cdot/$ denotes element by element division. Note that (65) requires none of the coordinates between $\mathbf{u}$ and $\mathbf{s}_1$ close to each other in order to obtain $\dot{\mathbf{u}}$. Should that not be the case, a different choice of the reference sensor or a simple rotation of the coordinate system would solve this problem.

VI. Simulations

This section presents three sets of simulations. The first set uses the geometry and settings from [17] for TDOA localization in 2D. The second set evaluates the performance for TDOA localization in 3D using randomly created geometries. The third set is for TDOA and FDOA localization of a moving source in 3D, also using randomly generated geometries. The number of ensemble runs L is 10 000 unless stated otherwise. The localization accuracy is assessed in terms of the mean-square error (MSE), $\mathrm{MSE} = \sum_{i=1}^{L} \|\mathbf{u}^{(i)} - \mathbf{u}^o\|^2/L$, and the bias, $\mathrm{bias} = \|\sum_{i=1}^{L}(\mathbf{u}^{(i)} - \mathbf{u}^o)\|/L$. The MSE and bias for the source velocity in TDOA and FDOA localization are defined in a similar manner. The proposed BiasSub and BiasRed methods are implemented as described at the end of Sections II and III. In particular, all the true values in the bias formula and constraint matrix are replaced by the estimated and noisy measurement values.

A. TDOA Localization in 2D

The sensor array has nine sensors. The first sensor, which is the reference for TDOA measurements, is at $[0, 0]^T$ m. The other eight sensors are distributed uniformly along a circle of radius 10 m, i.e., $\mathbf{s}_i = [10\cos(\frac{2\pi}{8}(i-1)), 10\sin(\frac{2\pi}{8}(i-1))]^T$m, $i = 2, 3, \ldots, 9$. The source is located at $\mathbf{u}^o = [100\cos\frac{2\pi}{32}, 100\sin\frac{2\pi}{32}]^T$ m. The TDOA noise is Gaussian and its covariance matrix is equal to the noise power times $(\mathbf{I} + \mathbf{1}\mathbf{1}^T)/2$, where $\mathbf{I}$ is an identity matrix and $\mathbf{1}$ is a vector of unity. Note that [17] uses a diagonal covariance matrix instead. At a given SNR, the noise power is obtained from (31) of [17] multiplied with the square of the signal propagation speed 3×10^8 m/s.

Fig. 1 compares the MSE of the proposed BiasSub and BiasRed methods. The solid line is the trace of the CRLB. Also included are the results from the weighted TLS (WTLS) method [17] and the MLE. The matrix $\mathbf{\Sigma}_L$ in the WTLS method is singular because we do not have sensor position error and a diagonal matrix with diagonal elements equal to 10^{-8} was added to $\mathbf{\Sigma}_L$ before taking inverse to form $\mathbf{W}_L$. The MLE is implemented by the Gauss-Newton iterations with the initial solution guess from grid search starting at the true source position. The grid resolution in a coordinate is the square root of the CRLB in that coordinate.

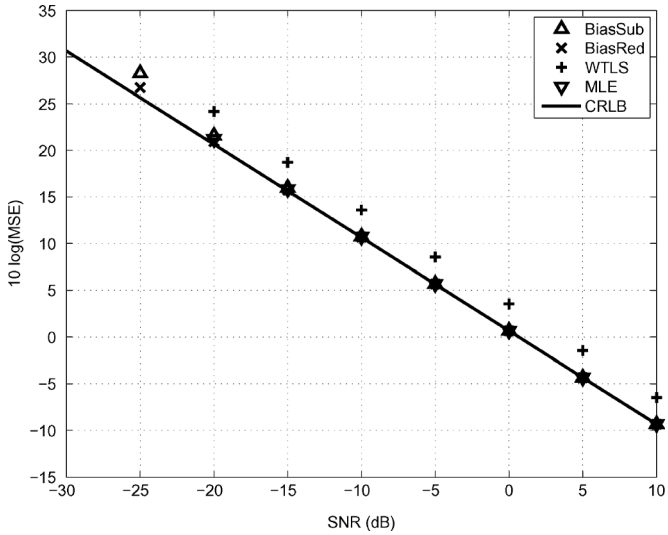

Fig. 1. Accuracy of TDOA source location estimates from various methods.

Fig. 1 indicates the two proposed methods achieve the CRLB accuracy very well when the SNR is not smaller than -20 dB. The MSE of the weighted minimum least-squares (WMLS) method, the terminology in [17] to denote closed-form solution from [1], is very close to BiasSub. We have the same observation as in [17] that the MSE performance of WTLS is higher than the CRLB, by about 3 dB in this case, no matter what value is the SNR. Fig. 2 presents the solution bias of the algorithms. The solid line is the theoretical bias of the WMLS method derived in Section II and it is in close agreement with the simulation result. The bias from BiasRed, WTLS and MLE are very close and they are about 20 dB less than that of WMLS before the thresholding effect takes place at about -20 dB SNR. Having bias very close to that of the MLE indicates BiasRed and WTLS are able to attain the bias as governed by the nonlinear nature of the localization problem. It is interesting that BiasSub can yield a much smaller bias. This is because it removes the bias caused by the nonlinear localization problem as well. However, BiasSub requires the exact knowledge of the noise covariance matrix whereas BiasRed and WTLS only need to know the structure of $\mathbf{Q}$.

$$\mathbf{\Omega} = E[\Delta\mathbf{A}^T\mathbf{W}_1\Delta\mathbf{A}] = \left[\begin{array}{c|c} \underbrace{\mathbf{O}_{2N\times 2N}}_{2N} & \underbrace{\mathbf{O}_{2N\times 3}}_{3} \\ \hline \mathbf{O}_{3\times 2N} & \tilde{\mathbf{\Omega}} \end{array}\right] \begin{matrix}\} 2N \\ \} 3\end{matrix} \tag{60}$$

and

$$\tilde{\mathbf{\Omega}} = 4\begin{bmatrix} \mathrm{tr}(\mathbf{W}_1\mathbf{Q}) & \mathrm{tr}(\mathbf{W}_1\mathbf{E}_{11}\mathbf{Q}) & \mathrm{tr}(\mathbf{W}_1\mathbf{E}_{12}\mathbf{Q}) \\ \mathrm{tr}\left(\mathbf{E}_{11}^T\mathbf{W}_1\mathbf{Q}\right) & \mathrm{tr}\left(\mathbf{E}_{11}^T\mathbf{W}_1\mathbf{E}_{11}\mathbf{Q}\right) & \mathrm{tr}\left(\mathbf{E}_{11}^T\mathbf{W}_1\mathbf{E}_{12}\mathbf{Q}\right) \\ \mathrm{tr}\left(\mathbf{E}_{12}^T\mathbf{W}_1\mathbf{Q}\right) & \mathrm{tr}\left(\mathbf{E}_{12}^T\mathbf{W}_1\mathbf{E}_{11}\mathbf{Q}\right) & \mathrm{tr}\left(\mathbf{E}_{12}^T\mathbf{W}_1\mathbf{E}_{12}\mathbf{Q}\right) \end{bmatrix}. \tag{61}$$

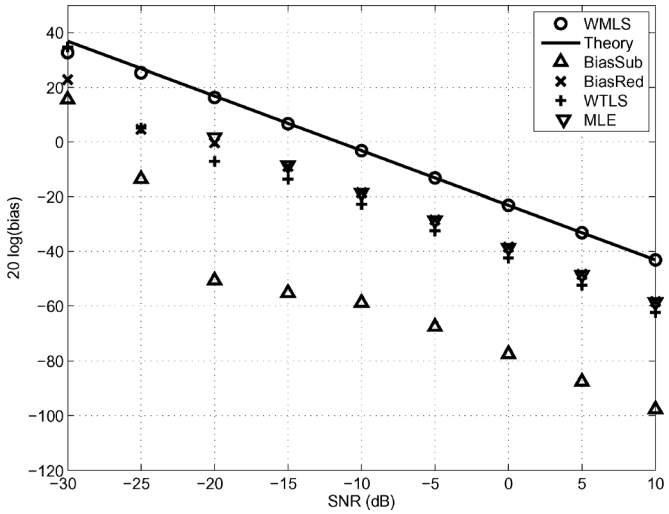

Fig. 2. Comparison of bias in TDOA source location estimates from different solution methods.

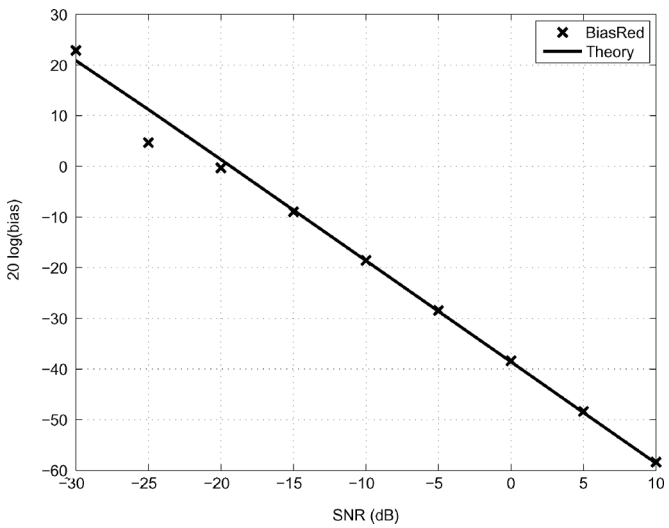

Fig. 3. Theoretical and simulation bias values of TDOA source location estimate from the BiasRed method.

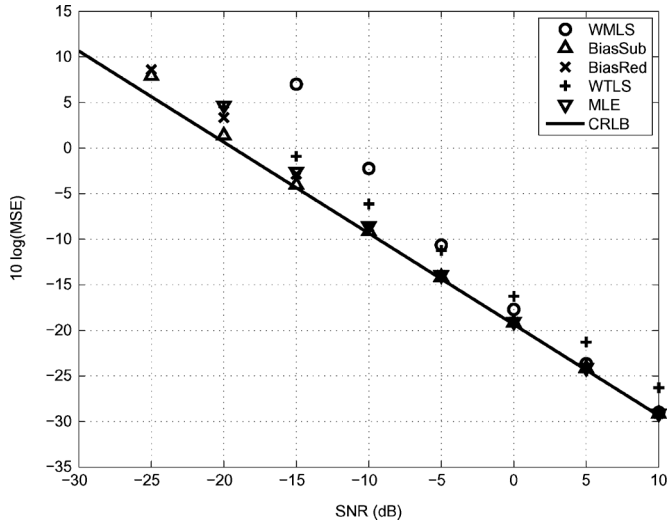

Fig. 4. TDOA source localization accuracy when averaging 100 independent solutions.

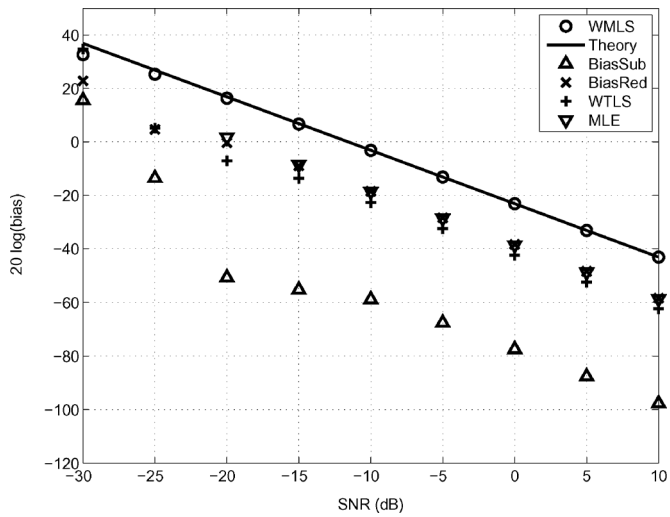

Fig. 5. Bias of TDOA source location estimates when averaging 100 independent solutions.

Fig. 3 confirms the theoretical analysis on the bias of BiasRed. The theoretical bias (solid line) matches very well with simulation when the SNR is not smaller than -20 dB.

We also produced the results when the final location estimate is obtained from the average of 100 independent solutions, which is used in [17] to illustrate the effect of bias in limiting the performance of WMLS. The number of ensemble runs is 1000. Figs. 4 and 5 give the results for MSE and bias. The inferior MSE performance of WMLS is obvious in this case. The estimates of BiasSub and BiasRed remain to reach the CRLB performance when the SNR is above -10 dB, and so does the MLE as expected. The accuracy of WTLS is worse than the CRLB. The bias results in Fig. 5 are basically the same as in Fig. 2 because averaging does not decrease bias.

Figs. 6–8 show the results as the target range increases from 0.5 to 20 times of the array radius. Both the MSE and bias increase with the target range. The observations remain the same as before that BiasSub and BiasRed achieve the CRLB accuracy and have bias much less than that of WMLS. The theoretical results also match very well with simulations, unless the source is very close or inside the sensor array.

B. TDOA Localization in 3D With Random Geometries

Two hundred localization geometries were created randomly using a uniformly distributed random number generator. Eight sensors are randomly placed with their distances to the origin not larger than 100. The source is randomly allocated with a distance between 100 and 600 from the origin. Fig. 9 shows the 200 geometries and the results presented are the average from those of these 200 geometries. For each geometry, the MSE and bias are obtained using 10 000 ensemble runs. The noise covariance matrix is equal to σ_r^2 in diagonal and $0.5\sigma_r^2$ otherwise, where σ_r^2 is the TDOA noise power multiplied by the square of the signal propagation speed.

Fig. 10 compares the MSE of the various algorithms as σ_r^2 increases and their bias values are shown in Fig. 11. Fig. 10 validates the optimum performance of BiasSub and BiasRed before the thresholding effect occurs at about $20\log(\sigma_r) = -5$.

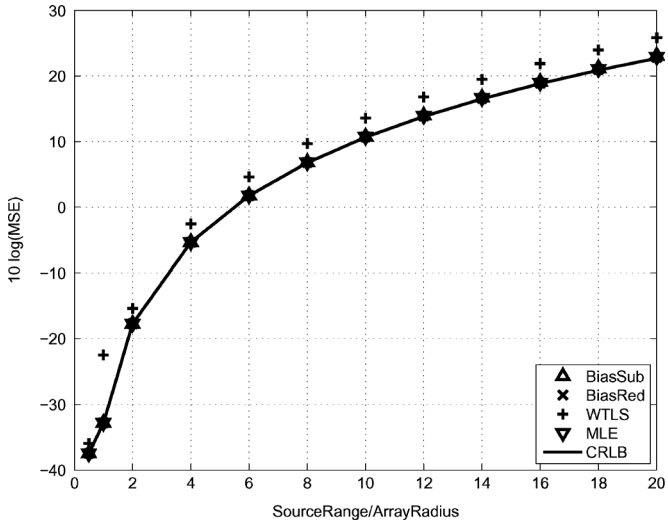

Fig. 6. TDOA source localization accuracy as the target range increases.

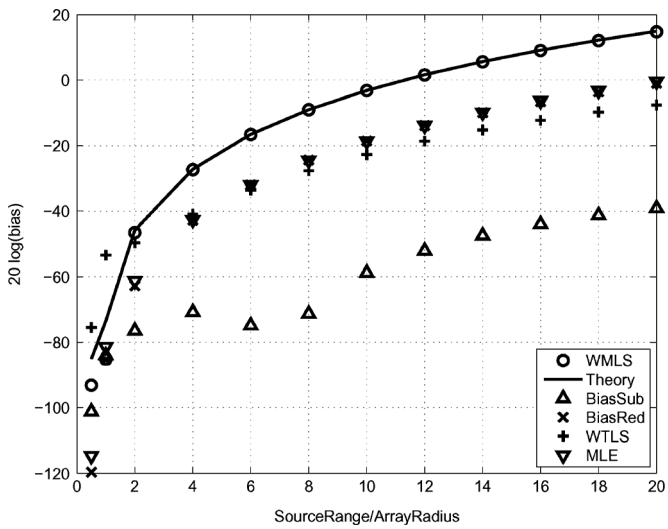

Fig. 7. Bias of TDOA source location estimates as the target range increases.

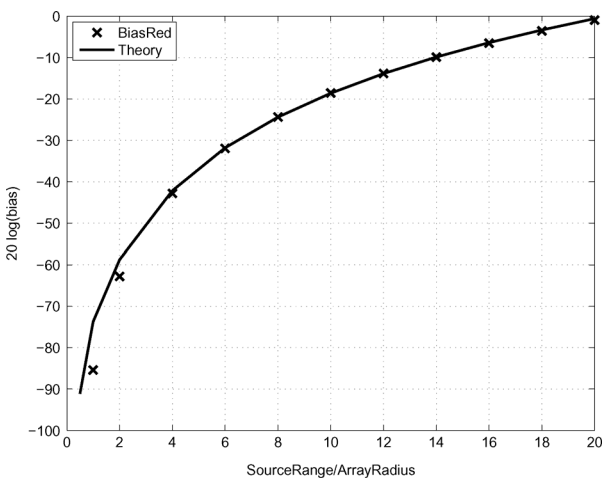

Fig. 8. Bias of the TDOA source location estimate from the BiasRed method as the target range increases.

Fig. 11 confirms the bias analysis of WMLS and BiasRed is able to lower the bias to the same level as the MLE. BiasSub is quite

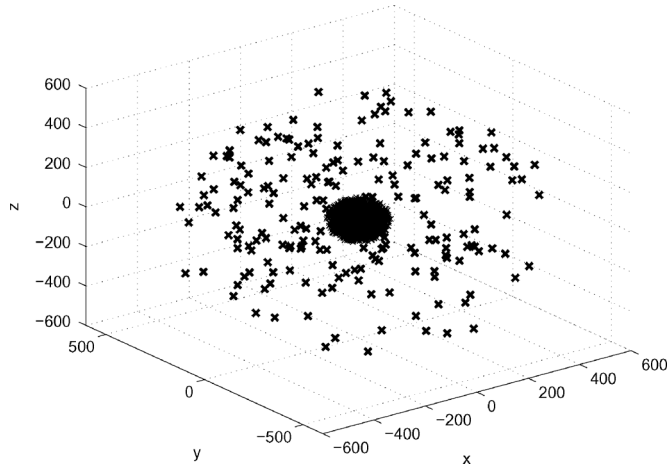

Fig. 9. The 200 random geometries for TDOA localization, the cross symbols represent the source locations and the sensors are within 100 units from the origin.

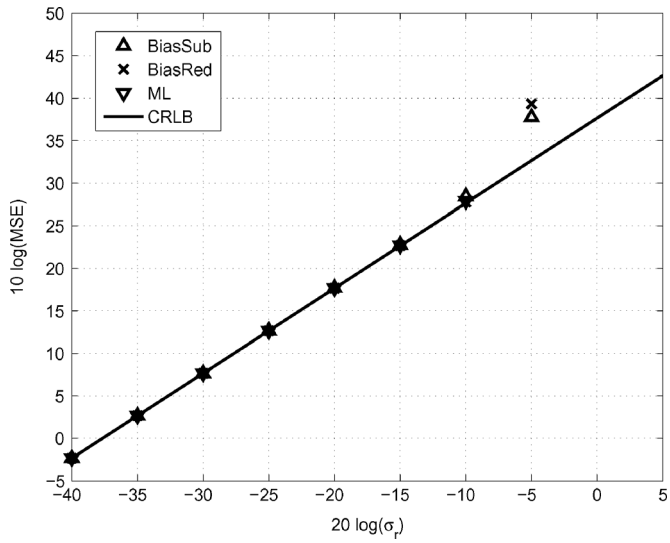

Fig. 10. Performance of various estimation methods under random geometries for TDOA localization.

effective in reducing the bias further. Fig. 12, again, corroborates the bias analysis of the BiasRed method.

C. TDOA and FDOA Localization in 3D With Random Geometries

Two hundred localization geometries were randomly created in the same manner as previous. Both the sensors and the source are moving and their velocities are generated randomly with the speeds not larger than 10 m/s. The TDOA covariance is the same as before and the FDOA covariance is 0.01 times that of TDOA. The TDOA and FDOA measurements are Gaussian distributed and they are uncorrelated with each other. Due to the large difference in the TDOA and FDOA noise powers, we apply diagonal loading to the constraint matrix $\tilde{\mathbf{\Omega}}$, where the loading factor is 10% of its trace. The purpose is to avoid poor rank of $\tilde{\mathbf{\Omega}}$ when the noise level becomes large. Figs. 13 and 14 give the MSE performance of the position and velocity estimates as σ_r^2 increases. The bias results are depicted in Figs. 15 and 16. They show the promising performance of the proposed BiasRed technique in reducing bias while maintaining the MSE performance close to

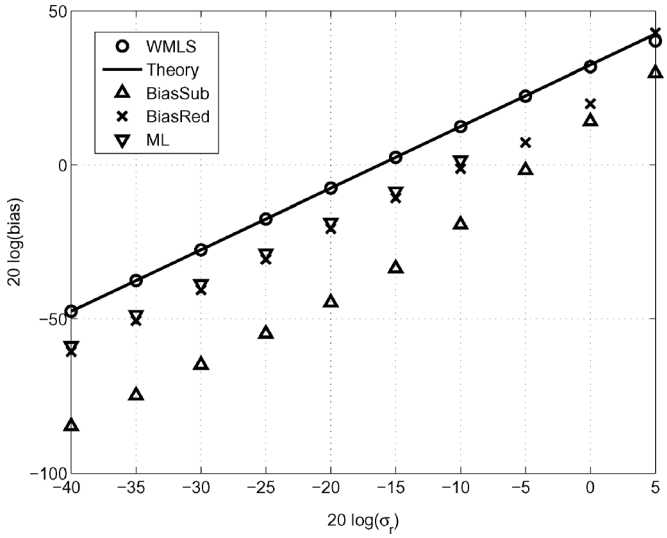

Fig. 11. Bias of source location estimates for TDOA localization.

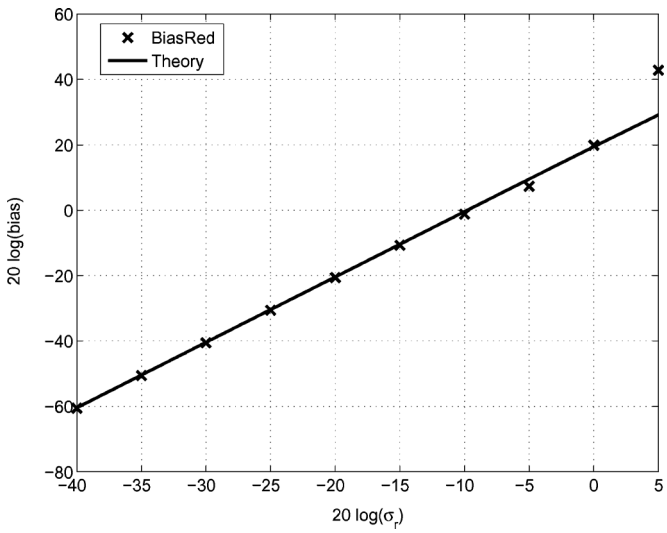

Fig. 12. Bias of the source location estimate obtained from the BiasRed method for TDOA localization.

the CRLB. It is noticed though the performance of BiasRed deviates from the CRLB a little earlier than WMLS. Improving the noise threshold of BiasRed is a subject for future research.

The same as in the original solution [1], the proposed methods assume a separate set of TDOA or TDOA/FDOA measurements is available for each individual source when multiple sources are present for localization. This can be achieved by exploring the disjointness in time or in frequency of the signals sent by different sources. The estimation of TDOAs and FDOAs for multiple source scenario is beyond what we would like to cover in this paper.

VII. Conclusion

This paper explores two methods to reduce the bias of the well-known closed-form TDOA positioning solution developed in [1]. The first method BiasSub subtracts the expected bias from the solution and the theoretical bias is derived for this method. The residual bias in BiasSub is very small and it mainly

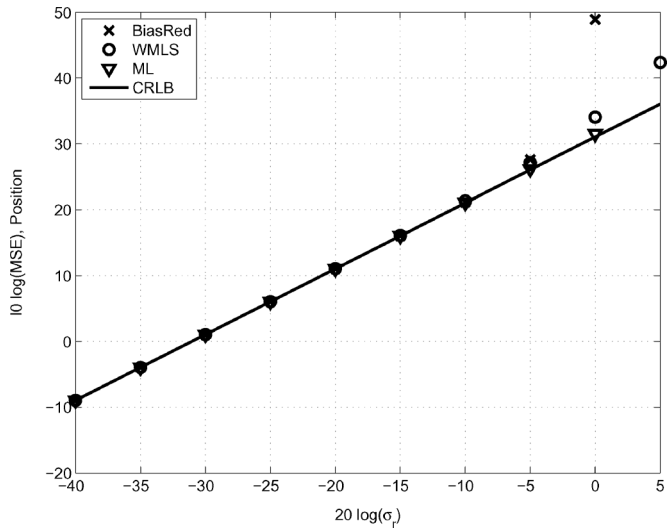

Fig. 13. Accuracy of source position estimates for TDOA and FDOA localization.

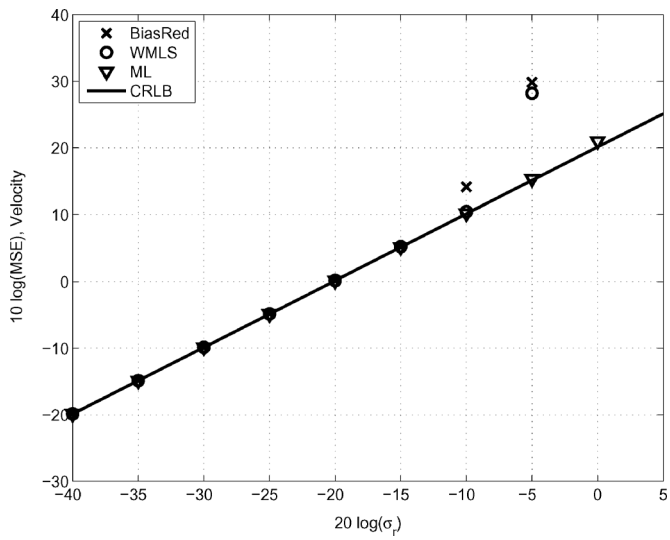

Fig. 14. Accuracy of source velocity estimates for TDOA and FDOA localization.

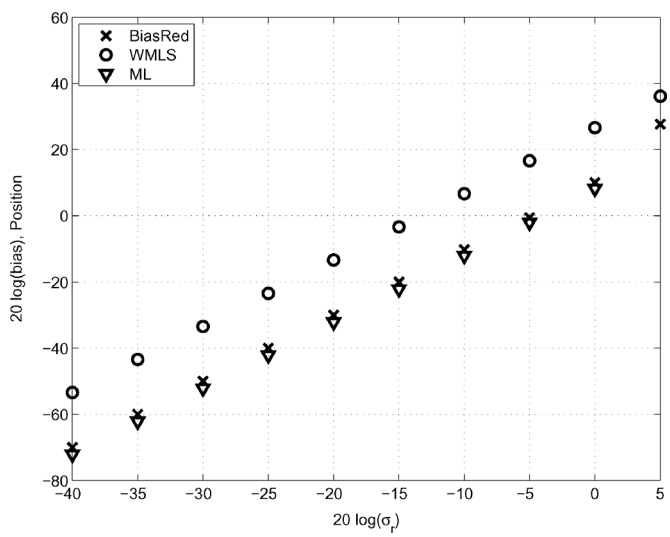

Fig. 15. Bias of source position estimates for TDOA and FDOA localization.

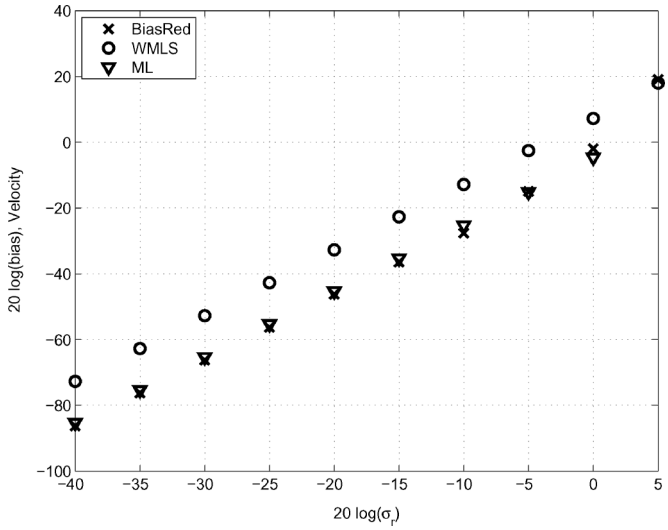

Fig. 16. Bias of source velocity estimates for TDOA and FDOA localization.

comes from the use of the solution estimate and noisy measurements in approximating the bias. The second method BiasRed expands the parameter space and imposes a quadratic constraint to reduce the bias. The bias of BiasRed is very close to that of the MLE which is resulted from the nonlinear nature of the localization problem itself. Both theoretical analysis and simulation studies validate the effectiveness of both methods in reducing the bias and achieving the CRLB performance under small Gaussian noise and distant signal source. They also outperform the WTLS solution which is not able to reach the CRLB accuracy. The BiasRed method is extended to reduce the position and velocity bias of a moving source for the closed-form solution of TDOA and FDOA positioning. The BiasSub method requires the covariance matrix of the measurements to be known perfectly to cancel out the bias and the BiasRed method only requires its structure. The proposed solutions remain to be in closed-form, are computationally attractive and do not require numerical search or SVD. They will be particularly useful in the situations where bias could dominate performance such as in UWB localization or in target tracking.

The work presented here does not consider sensor position error to simplify the illustration. Extension of the proposed solutions to include sensor position errors is a subject for further study.

Appendix I

Let $\mathbf{P}_1$ be $(\mathbf{G}_1^T\mathbf{W}_1\mathbf{G}_1)$ and (11) becomes

$$\Delta\boldsymbol{\varphi}_1 = \mathbf{P}_1^{-1}\mathbf{G}_1^T\mathbf{W}_1(\mathbf{B}_1\mathbf{n} + \mathbf{n}\odot\mathbf{n}) \tag{66}$$

where $\mathbf{B}_1$ is defined in (6). $\mathbf{G}_1$ can be expressed as

$$\mathbf{G}_1 = \mathbf{G}_1^o + \Delta\mathbf{G}_1 \tag{67}$$

$$\Delta\mathbf{G}_1 = -2\left[\mathbf{O}_{(M-1)\times N}, \mathbf{n}\right] \tag{68}$$

and $\mathbf{n}$ is the measurement noise vector. Using (67) gives

$$\begin{aligned}\mathbf{P}_1 &\approx \mathbf{P}_1^o + \Delta\mathbf{P}_1\\ \mathbf{P}_1^o &= \mathbf{G}_1^{oT}\mathbf{W}_1\mathbf{G}_1^o\\ \Delta\mathbf{P}_1 &= \mathbf{G}_1^{oT}\mathbf{W}_1\Delta\mathbf{G}_1 + \Delta\mathbf{G}_1^T\mathbf{W}_1\mathbf{G}_1^o.\end{aligned} \tag{69}$$

The term $\Delta\mathbf{G}_1^T\mathbf{W}_1\Delta\mathbf{G}_1$ is relatively insignificant and is neglected. When the noise level is small, we have from the Neumann expansion [28]

$$\begin{aligned}\mathbf{P}_1^{-1} &\approx \left(\mathbf{I} + \mathbf{P}_1^{o-1}\Delta\mathbf{P}_1\right)^{-1}\mathbf{P}_1^{o-1}\\ &\approx \left(\mathbf{I} - \mathbf{P}_1^{o-1}\Delta\mathbf{P}_1\right)\mathbf{P}_1^{o-1}.\end{aligned} \tag{70}$$

Putting (67) and (70) into (66) and keeping up to second-order noise terms only yield

$$\begin{aligned}\Delta\boldsymbol{\varphi}_1 \approx \mathbf{H}_1\mathbf{B}_1\mathbf{n} + \mathbf{H}_1\mathbf{n}\odot\mathbf{n} + \mathbf{P}_1^{o-1}\Delta\mathbf{G}_1^T\mathbf{W}_1\mathbf{B}_1\mathbf{n}\\ -\mathbf{P}_1^{o-1}\Delta\mathbf{P}_1\mathbf{H}_1\mathbf{B}_1\mathbf{n}\end{aligned} \tag{71}$$

where $\mathbf{H}_1$ is defined in (13). Since $E[\mathbf{n}\mathbf{n}^T] = \mathbf{Q}$, using (68) gives

$$E\left[\Delta\mathbf{G}_1^T\mathbf{W}_1\mathbf{B}_1\mathbf{n}\right] = -2\begin{bmatrix}\mathbf{0}_{N\times 1}\\ \mathrm{tr}(\mathbf{W}_1\mathbf{B}_1\mathbf{Q})\end{bmatrix}.$$

Also

$$E\left[\Delta\mathbf{G}_1\mathbf{H}_1\mathbf{B}_1\mathbf{n}\right] = -2\mathbf{Q}\mathbf{B}_1\mathbf{H}_1(N+1,:)^T$$

and

$$E\left[\Delta\mathbf{G}_1^T\mathbf{W}_1\mathbf{G}_1^o\mathbf{H}_1\mathbf{B}_1\mathbf{n}\right] = -2\begin{bmatrix}\mathbf{0}_{N\times 1}\\ \mathrm{tr}\left(\mathbf{W}_1\mathbf{G}_1^o\mathbf{H}_1\mathbf{B}_1\mathbf{Q}\right)\end{bmatrix}$$

where $\mathbf{H}_1(N+1,:)$ is the last row of $\mathbf{H}_1$.

Hence, after substituting (69) into (70) and taking expectation result in the bias formula (12) of $\boldsymbol{\varphi}_1$.

Appendix II

The error of $\boldsymbol{\varphi}_2$ is (14). Although $\mathbf{G}_2$ is constant, $\mathbf{W}_2$ is formed using $\boldsymbol{\varphi}_1$ and it contains noise. We shall first express $\mathbf{W}_2$ from (9) in terms of $\mathbf{n}$ and $\Delta\boldsymbol{\varphi}_1$. $\mathbf{B}_2$ can be expressed as, after representing $\boldsymbol{\varphi}_1$ as $\boldsymbol{\varphi}_1^o + \Delta\boldsymbol{\varphi}_1$,

$$\begin{aligned}\mathbf{B}_2 &= \mathbf{B}_2^o + \Delta\mathbf{B}_2\\ \Delta\mathbf{B}_2 &= 2\,\mathrm{diag}\{\Delta\boldsymbol{\varphi}_1\}.\end{aligned} \tag{72}$$

Under the conditions that the measurement noise is small and the source is not close to any sensors so that $\mathbf{B}_2^{o-1}\Delta\mathbf{B}_2 \approx \mathbf{O}$, we have the approximation [28]

$$\begin{aligned}\mathbf{B}_2^{-1} &= \left(\mathbf{I} + \mathbf{B}_2^{o-1}\Delta\mathbf{B}_2\right)^{-1}\mathbf{B}_2^{o-1}\\ &\approx \mathbf{B}_2^{o-1} - \mathbf{B}_2^{o-1}\Delta\mathbf{B}_2\mathbf{B}_2^{o-1}.\end{aligned}$$

Putting (69) and (72) into (9) and keeping the error terms up to second-order yield

$$\begin{aligned}\mathbf{W}_2 &\approx \mathbf{W}_2^o + \Delta\mathbf{W}_2\\ \Delta\mathbf{W}_2 &= \mathbf{B}_2^{o-1}\Delta\mathbf{P}_1\mathbf{B}_2^{o-1} - \mathbf{B}_2^{o-1}\Delta\mathbf{B}_2\mathbf{W}_2^o - \mathbf{W}_2^o\mathbf{B}_2^{o-1}\Delta\mathbf{B}_2.\end{aligned} \tag{73}$$

Note that $\Delta\mathbf{B}_2\mathbf{B}_2^{o-1} = \mathbf{B}_2^{o-1}\Delta\mathbf{B}_2$ because $\Delta\mathbf{B}_2$ and $\mathbf{B}_2^{o-1}$ are diagonal matrices. Let us denote $\mathbf{G}_2^T\mathbf{W}_2\mathbf{G}_2$ as $\mathbf{P}_2$ for notation simplicity. Then

$$\begin{aligned}\mathbf{P}_2 &= \mathbf{P}_2^o + \Delta\mathbf{P}_2\\ \Delta\mathbf{P}_2 &= \mathbf{G}_2^T\Delta\mathbf{W}_2\mathbf{G}_2.\end{aligned}$$

Again, with sufficiently small noise level so that $\mathbf{P}_2^{o\,-1}\Delta\mathbf{P}_2 \approx \mathbf{O}$, the approximation

$$\mathbf{P}_2^{-1} \approx \left(\mathbf{I} - \mathbf{P}_2^{o\,-1}\Delta\mathbf{P}_2\right)\mathbf{P}_2^{o\,-1} \tag{74}$$

holds.

If we use (74) into (14) and ignore the noise terms higher than second order, the bias of $\boldsymbol{\varphi}_2$ is

$$E[\Delta\boldsymbol{\varphi}_2] \approx \mathbf{H}_2\left(\mathbf{c}_1 + \mathbf{B}_2^o E[\Delta\boldsymbol{\varphi}_1]\right) + \mathbf{P}_2^{o\,-1}\mathbf{G}_2^T E\left[\Delta\mathbf{W}_2\mathbf{P}_3\mathbf{B}_2^o\Delta\boldsymbol{\varphi}_1\right] \tag{75}$$

where $\mathbf{H}_2$ is given by (16)

$$\mathbf{P}_3 = (\mathbf{I} - \mathbf{G}_2\mathbf{H}_2)$$

and $\mathbf{c}_1$ is defined below (16). After substituting (73), we have

$$E\left[\Delta\mathbf{W}_2\mathbf{P}_3\mathbf{B}_2^o\Delta\boldsymbol{\varphi}_1\right] = \boldsymbol{\alpha} + \boldsymbol{\beta} + \boldsymbol{\gamma}.$$

The value of $\boldsymbol{\alpha}$ is, upon using (69) and (71) and keeping only second-order noise terms

$$\begin{aligned}\boldsymbol{\alpha} &= E\left[\mathbf{B}_2^{o\,-1}\Delta\mathbf{P}_1\mathbf{B}_2^{o\,-1}\mathbf{P}_3\mathbf{B}_2^o\Delta\boldsymbol{\varphi}_1\right] \\ &= -2\mathbf{B}_2^{o\,-1}\left(\mathbf{G}_1^{o\,T}\mathbf{W}_1\mathbf{Q}\mathbf{P}_4(M-1,:)^T + \begin{bmatrix}\mathbf{0}_{N\times 1} \\ \operatorname{tr}(\mathbf{W}_1\mathbf{G}_1^o\mathbf{P}_4\mathbf{Q})\end{bmatrix}\right)\end{aligned} \tag{76}$$

where

$$\mathbf{P}_4 = \mathbf{B}_2^{o\,-1}\mathbf{P}_3\mathbf{B}_2^o\mathbf{H}_1\mathbf{B}_1^o$$

and $\mathbf{H}_1$ is defined in (13). Also, from (72),

$$\boldsymbol{\beta} = -E\left[\mathbf{B}_2^{o\,-1}\Delta\mathbf{B}_2\mathbf{W}_2^o\mathbf{P}_3\mathbf{B}_2^o\Delta\boldsymbol{\varphi}_1\right] = -2\mathbf{B}_2^{o\,-1}\mathbf{p}_{5,W2} \tag{77}$$

$$\boldsymbol{\gamma} = -E\left[\mathbf{W}_2^o\mathbf{B}_2^{o\,-1}\Delta\mathbf{B}_2\mathbf{P}_3\mathbf{B}_2^o\Delta\boldsymbol{\varphi}_1\right] = -2\mathbf{W}_2^o\mathbf{B}_2^{o\,-1}\mathbf{p}_5 \tag{78}$$

where $\mathbf{p}_{5,W2}$ and $\mathbf{p}_5$ denote column vectors formed by the diagonal elements of $\mathbf{W}_2^o\mathbf{P}_5$ and $\mathbf{P}_5$,

$$\mathbf{P}_5 = \mathbf{P}_3\mathbf{B}_2^o\mathbf{C}_1$$

and $\mathbf{C}_1$ is defined in (17). Consequently, we have the bias formula (15) of $\boldsymbol{\varphi}_2$.

Appendix III

We would like to find the explicit solution of $\mathbf{v}_2$ for TDOA and FDOA positioning from (42) without using the generalized eigen-decomposition, where $\mathbf{v}_2$ is 3×1. Let $\operatorname{adj}(\tilde{\boldsymbol{\Omega}})$ and $\det(\tilde{\boldsymbol{\Omega}})$ be the adjoint and determinant of $\tilde{\boldsymbol{\Omega}}$ so that $\tilde{\boldsymbol{\Omega}}^{-1} = \operatorname{adj}(\tilde{\boldsymbol{\Omega}})/\det(\tilde{\boldsymbol{\Omega}})$. We can rewrite (42) as

$$\mathbf{F}\mathbf{v}_2 = \tilde{\lambda}\mathbf{v}_2 \tag{79}$$

where $\mathbf{F} = \operatorname{adj}(\tilde{\boldsymbol{\Omega}})(\mathbf{A}_{22} - \mathbf{A}_{12}^T\mathbf{A}_{11}^{-1}\mathbf{A}_{12})$, $\tilde{\lambda} = \lambda\det(\tilde{\boldsymbol{\Omega}})$ and $\tilde{\lambda}$ is the smallest eigenvalue of $\mathbf{F}$. To obtain $\tilde{\lambda}$, we equate $\det(\tilde{\lambda}\mathbf{I} - \mathbf{F})$ to zero which gives the third-order polynomial

$$\tilde{\lambda}^3 + a\tilde{\lambda}^2 + b\tilde{\lambda} + c = 0 \tag{80}$$

where

$$\begin{aligned}a &= -(f_{11} + f_{22} + f_{33}), \\ b &= (f_{11}f_{22} + f_{11}f_{33} + f_{22}f_{33}) \\ &\quad - (f_{12}f_{21} + f_{23}f_{32} + f_{13}f_{31}), \\ c &= (f_{11}f_{23}f_{32} + f_{22}f_{13}f_{31} + f_{33}f_{12}f_{21}) \\ &\quad - (f_{11}f_{22}f_{33} + f_{12}f_{23}f_{31} + f_{13}f_{21}f_{32})\end{aligned}$$

and f_{ij} is the (i,j)th element of $\mathbf{F}$. The roots of (80) have analytic form as shown in Appendix IV. After determining the minimum root $\tilde{\lambda}_{\min}$ of the polynomial, we form

$$\tilde{\mathbf{F}} = (\mathbf{F} - \tilde{\lambda}_{\min}\mathbf{I}) = \begin{bmatrix}\tilde{\mathbf{F}}_{11} & \tilde{\mathbf{F}}_{12} \\ \tilde{\mathbf{F}}_{21} & \tilde{\mathbf{F}}_{22}\end{bmatrix}\begin{matrix}\}\,2 \\ \}\,1.\end{matrix}$$

From (79), $\mathbf{v}_2(1:2) = -\tilde{\mathbf{F}}_{11}^{-1}\tilde{\mathbf{F}}_{12}\cdot v_2(3)$ and hence

$$\mathbf{v}_2 = \begin{bmatrix}-\tilde{\mathbf{F}}_{11}^{-1}\tilde{\mathbf{F}}_{12} \\ 1\end{bmatrix} v_2(3) \tag{81}$$

where $v_2(3)$ is a scaling factor whose specific value is irrelevant when converting $\mathbf{v}$ to $\boldsymbol{\varphi}_1$.

Appendix IV
Explicit Formulas for the Roots of a Third-Order Polynomial

We are interested in finding the roots of the third-order polynomial:

$$f(x) = x^3 + ax^2 + bx + c. \tag{82}$$

For convenience purpose, let us define the intermediate values

$$\begin{aligned}q &= \frac{1}{9}(3b - a^2), \\ r &= \frac{1}{54}(9ab - 27c - 2a^3), \\ \Delta &= q^3 + r^2.\end{aligned} \tag{83}$$

i) If $\Delta \geq 0$, there are one real and two complex roots. The real root is

$$x_1 = -\frac{a}{3} + (s+t) \tag{84}$$

where

$$s = (r + \Delta^{1/2})^{1/3}, \quad t = (r - \Delta^{1/2})^{1/3}.$$

ii) If $\Delta < 0$, all three roots are real and they are

$$\begin{aligned}x_1 &= -\frac{a}{3} + 2\rho^{1/3}\cos(\theta/3), \\ x_2 &= -\frac{a}{3} - \rho^{1/3}\cos(\theta/3) - \sqrt{3}\rho^{1/3}\sin(\theta/3) \\ x_3 &= -\frac{a}{3} - \rho^{1/3}\cos(\theta/3) + \sqrt{3}\rho^{1/3}\sin(\theta/3)\end{aligned} \tag{85}$$

where

$$\rho = \sqrt{-q^3}, \;\; \theta = \cos^{-1}\left(\frac{r}{\rho}\right).$$

ACKNOWLEDGMENT

The author would like to thank the anonymous reviewers for providing very constructive comments and suggestions that have resulted in improving the quality of the paper.

REFERENCES

[1] Y. T. Chan and K. C. Ho, "A simple and efficient estimator for hyperbolic location," *IEEE Trans. Signal Process.*, vol. 42, pp. 1905–1915, Aug. 1994.
[2] E. Weinstein, "Optimal source localization and tracking from passive array measurements," *IEEE Trans. Acoust., Speech, Signal Process.*, vol. ASSP-30, pp. 69–76, Feb. 1982.
[3] N. Patwari, J. N. Ash, S. Kyperountas, A. O. Hero, III, R. L. Moses, and N. S. Correal, "Locating the nodes: Cooperative localization in wireless sensor networks," *IEEE Signal Process. Mag.*, vol. 22, pp. 54–69, Jul. 2005.
[4] A. H. Sayed, A. Tarighat, and N. Khajehnouri, "Network-based wireless location: Challenges faced in developing techniques for accurate wireless location information," *IEEE Signal Process. Mag.*, vol. 22, pp. 24–40, Jul. 2005.
[5] S. Coraluppi, "Multistatic sonar localization," *IEEE J. Ocean. Eng.*, vol. 31, pp. 964–974, Oct. 2006.
[6] F. Ahmad and M. Amin, "Noncoherent approach to through-the-wall radar localization," *IEEE Trans. Aerosp. Electron. Syst.*, vol. 42, pp. 1405–1419, Oct. 2006.
[7] K. W. K. Lui, W. K. Ma, H. C. So, and F. K. W. Chan, "Semi-definite programming algorithms for sensor network node localization with uncertainties in anchor positions and/or propagation speed," *IEEE Trans. Signal Process.*, vol. 57, pp. 752–763, Feb. 2009.
[8] U. A. Khan, S. Kar, and J. M. F. Moura, "Distributed sensor localization in random environments using minimal number of anchor nodes," *IEEE Trans. Signal Process.*, vol. 57, pp. 2000–2016, May 2009.
[9] K. Yang, G. Wang, and Z. Q. Luo, "Efficient convex relaxation methods for robust target localization by a sensor network using time differences of arrivals," *IEEE Trans. Signal Process.*, vol. 57, pp. 2775–2784, July 2009.
[10] P. Addesso, S. Marano, and V. Matta, "Estimation of target location via likelihood approximation in sensor networks," *IEEE Trans. Signal Process.*, vol. 58, pp. 1358–1368, Mar. 2010.
[11] U. A. Khan, S. Kar, and J. M. F. Moura, "DILAND: An algorithm for distributed sensor localization with noisy distance measurements," *IEEE Trans. Signal Process.*, vol. 58, pp. 1940–1947, Mar. 2010.
[12] A. Amar and A. J. Weiss, "Localization of narrowband radio emitters based on Doppler frequency shifts," *IEEE Trans. Signal Process.*, vol. 56, pp. 5500–5508, Nov. 2008.
[13] A. J. Weiss, "Direct geolocation of wideband emitters based on delay and Doppler," *IEEE Trans. Signal Process.*, vol. 59, pp. 2513–2521, June 2011.
[14] W. H. Foy, "Position-location solutions by Taylor-series estimation," *IEEE Trans. Aerosp. Electron. Syst.*, vol. AES-12, pp. 187–194, Mar. 1976.
[15] A. Beck, P. Stoica, and J. Li, "Exact and approximate solutions of source localization problems," *IEEE Trans. Signal Process.*, vol. 56, pp. 1770–1778, May 2008.
[16] S. M. Kay, *Fundamentals of Statistical Signal Processing, Estimation Theory*. Englewood Cliffs, NJ: Prentice-Hall, 1993.
[17] R. J. Barton and D. Rao, "Performance capabilities of long-range UWB-IR TDOA localization systems," *EURASIP J. Adv. Signal Process.*, vol. 2008, 2008.
[18] H. W. Wei, Q. Wan, Z. X. Chen, and S. F. Ye, "A novel weighted multidimensional scaling analysis for time-of-arrival-based mobile location," *IEEE Trans. Signal Process.*, vol. 56, pp. 3018–3022, Jul. 2008.
[19] K. Lui, F. Chan, and H. C. So, "Semidefinite programming approach for range-difference based source localization," *IEEE Trans. Signal Process.*, vol. 57, pp. 1630–1633, Apr. 2009.
[20] K. Dogancay, "Bias compensation for the bearings-only pseudolinear target track estimator," *IEEE Trans. Signal Process.*, vol. 54, pp. 59–68, Jan. 2006.
[21] Y. Huang, J. Benesty, G. W. Elko, and R. M. Mersereati, "Real-time passive source localization: A practical linear-correction least-squares approach," *IEEE Trans. Speech, Audio Process.*, vol. 9, pp. 943–956, Nov. 2001.
[22] K. Yang, J. An, and Z. Xu, "A quadratic constraint total least-squares algorithm for hyperbolic location," *Int. J. Commun., Network, Syst. Sci.*, pp. 130–135, 2008.
[23] X. Sun, J. Li, P. Huang, and J. Pang, "Total least-squares solution of active target localization using TDOA and FDOA measurements in WSN," in *Proc. IEEE 22nd Int. Conf. on Adv. Inf. Netw. Appl. Workshops (AINAW 2008)*, Okinawa, Japan, Mar. 2008, pp. 995–999.
[24] K. C. Ho and W. Xu, "An accurate algebraic solution for moving source location using TDOA and FDOA measurements," *IEEE Trans. Signal Process.*, vol. 52, pp. 2453–2463, Sep. 2004.
[25] H. W. Wei, R. Peng, Q. Wan, Z. X. Chen, and S. F. Ye, "Multidimensional scaling analysis for passive moving target localization with TDOA and FDOA measurements," *IEEE Trans. Signal Process.*, vol. 58, pp. 1677–1688, Mar. 2010.
[26] S. Goldberger, *Econometric Theory*. New York: Wiley, 1964.
[27] K. C. Ho and Y. T. Chan, "An asymptotically unbiased estimator for bearings-only and Doppler-bearing target motion analysis," *IEEE Trans. Signal Process.*, vol. 54, pp. 809–822, Mar. 2006.
[28] T. K. Moon and W. C. Stirling, *Mathematical Methods and Algorithms for Signal Processing*. Upper Saddle River, NJ: Prentice-Hall, 2000.

K. C. Ho (M'91–SM'00–F'09) was born in Hong Kong. He received the B.Sc. degree with First Class Honors in electronics in 1988 and the Ph.D. degree in electronic engineering in 1991 from the Chinese University of Hong Kong.

He was a Research Associate with the Royal Military College of Canada from 1991 to 1994. He joined the Bell-Northern Research, Montreal, Canada, in 1995 as a member of scientific staff. He was a faculty member of the Department of Electrical Engineering, University of Saskatchewan, Saskatoon, Canada, from September 1996 to August 1997. Since September 1997, he has been with the University of Missouri and where he is currently a Professor in the Electrical and Computer Engineering Department. His research interests are in sensor array processing, source localization, subsurface object detection, wireless communications, and the development of efficient adaptive signal processing algorithms for various applications. He is an inventor of five United States patents, three Canadian patents, two patents in Europe, and five patents in Asia on geolocation, mobile communications, and signal processing.

Dr. Ho is the Rapporteur of ITU-T Q15/SG16: Voice Gateway Signal Processing Functions and Circuit Multiplication Equipment/Systems. He is the Editor of the ITU-T Standard Recommendations G.160: Voice Enhancement Devices and G.168: Digital Network Echo Cancellers. He is the Vice-Chair of the Sensor Array and Multichannel Technical Committee in the IEEE Signal Processing Society. He was an Associate Editor of the IEEE SIGNAL PROCESSING LETTERS from 2004 to 2008, an Associate Editor of the IEEE TRANSACTIONS ON SIGNAL PROCESSING from 2003 to 2006, and is serving his second (since January 2009) Associate Editor term with the IEEE TRANSACTIONS ON SIGNAL PROCESSING. He received the Junior Faculty Research Award in 2003 and the Senior Faculty Research Award in 2009 from the College of Engineering at the University of Missouri.